Chloride-induced depassivation and corrosion of mild steel in magnesium potassium phosphate cement

Wang, Danqian; Yue, Yanfei; Xie, Zhichao; Mi, Tangwei; Yang, Siyu; McCague, Colum

DOI:
10.1016/j.corsci.2022.110482

Publication date:
2022

Chloride-induced depassivation and corrosion of mild steel in magnesium potassium phosphate cement

Danqian Wang[1,2], Yanfei Yue[1*], Zhichao Xie[1], Tangwei Mi[2], Siyu Yang[2], Colum McCague[3,2], Jueshi Qian[1], Yun Bai[2**]

1 College of Materials Science and Engineering, Chongqing University, Chongqing 400045, PR China

2 Advanced & Innovative Materials (AIM) Group, Department of Civil, Environmental and Geomatic Engineering, University College London, London, UK, WC1E 6BT

3 Mineral Products Association, Gillingham House, 38-44 Gillingham Street, London, UK, SW1V 1HU

Corresponding author's email address: * yanfei.yue@cqu.edu.cn; ** yun.bai@ucl.ac.uk

Abstract

This study investigated the chloride-induced depassivation and corrosion of mild steel in the magnesium potassium phosphate cement (MKPC) pore solutions at different magnesia-to-phosphate (M/P) ratios via several electrochemical methods and surface characterizations. Results showed that although the pH of MKPC is much lower than that of PC, the corrosion resistance of mild steel is significantly higher, with critical chloride values in MKPC being several orders higher than that in PC. Chloride-induced corrosion resistance increases with increasing M/P ratios. Whilst both pH and HPO_4^{2-}/PO_4^{3-} ions influence the formation of corrosion products, the pH plays a dominant role in the corrosion resistance.

Key words: Chloride-induced corrosion; magnesium phosphate cement; mild steel; magnesia-to-phosphate ratio

1 Introduction

The alkaline environment of Portland cement (PC), which is usually around pH 13, favours the formation of a protective layer, so called passive film, on the surface of reinforcing steel [1]. A good quality of passive film can improve the durability of reinforced concrete structure by providing protection to the steel against the deterioration caused by corrosion. It has been well-established that the passivation process involves the electrochemical and chemical reactions between reinforcing steel and concrete pore solution, which results in the formation of a thermodynamically stable film, typically consisting of an outer layer of Fe(III) oxides and an inner layer of Fe(II) oxides [2]. However, the protective capacity of this oxide film can be destroyed in a low pH environment or by the presence of chloride ions in concrete pore solutions [3, 4]. According to previous research in the literature, when the pH of the concrete pore solution is below c.a. 10.5, the depassivation of the passive film is initiated and a porous and less protective oxide film consisting of FeOOH can form on the surface of mild steel, making it more vulnerable to the chloride-induced attack [5]. Alternatively, when the concentration of chloride ion on the surface of steel is above a critical value, the defective areas of the passive film could be damaged, and this can result in the pitting corrosion of steel. It should be noted that the pitting corrosion, in turn, can promote the dissolution of Fe from the steel substrate and the dissolved Fe ions may subsequently react with the hydroxyl ions in solution, forming some corrosion products consisting of iron oxide and hydroxide at the steel/concrete interface [6, 7]. As a result, the bond between steel and concrete could be reduced due to the formation of these porous and expansive corrosion products, which can cause severe durability, even safety, problems of reinforced structures [8]. To ensure concrete, in particular the cover concrete, can provide adequate protection to reinforcing steel, limiting factors such as minimum cement content, maximum water-to-cement (W/C) ratio and suitable binder compositions, have been specified in different codes for PC-based concrete [9, 10]. Additionally, the threshold values of chloride have also been specified for the design and service life prediction purposes for PC-based concretes.

In recent years, non-PC based cementitious materials, such as magnesium potassium phosphate cement (MKPC), have been gaining increased popularity in the construction industry. Compared to PC system, MKPC has demonstrated high early strength, quick setting, good bond to the existing concrete, high volume stability and good resistance to abrasion [11]. It has thus been increasingly used as a rapid repair material for concrete structures [12], potential binder for seawater concrete [13, 14] and matrices for nuclear waste immobilisation [15]. However, unlike PC which is a precision engineered commercial product with targeted range of minerals, MKPC is usually formulated with a soluble phosphate (e.g. KH_2PO_4) and dead burnt magnesium oxide (MgO) at varying MgO-to-KH_2PO_4 (M/P) molar ratios for different applications, even though in theory a stoichiometric 1:1 M/P molar ratio should be adopted (as shown in Eq. 1). Since the reaction of MKPC is considered to be a neutralisation reaction between MgO and phosphates, the pH of the MKPC pore solution, which increases with the increase of M/P, is reported to be in the range of pH 8 to 12. Obviously, these pH values are lower (even much lower) than that of the PC system and the potential application of MKPC as a binder in reinforced concrete has thus been questioned. This is because with this low pH value, concerns might have been raised over the quality of the passive film formed on reinforcing steel as well as its ability to resist the carbonation and chloride-induced attacks to reinforcing steel. However, the previous study carried out by the authors showed that comparable or even better passive films can be formed on the reinforcing steel embedded in MKPC matrices in comparison with PC, even though the pH values are lower than that of the PC. Moreover, the passivity of reinforcing steel was found to increase with increasing M/P ratios from 7 to 17 [16]. It is, therefore, reasonable to postulate that the resistance of the reinforcing steel embedded in MKPC to chloride-induced attack should be comparable or even better than that in PC. [17, 18]. However, due to the complex nature of MKPC, its possible effects on the passivation and depassivation of reinforcing steel is also complicated (as detailed below).

$$MgO + KH_2PO_4 + 5H_2O \rightarrow MgKPO_4.6H_2O \quad \text{Eq. 1}$$

As highlighted before, a ratio higher than the stoichiometric 1:1 M/P molar ratio is often required in practice in order to achieve the desired properties, in particular the strength property, of MKPC concrete. As a result, the M/P ratios often vary significantly in different applications, which in turn can influence the hydration process [19], pore solution chemistry [16] as well as mechanical properties [20]. Most importantly, as the M/P ratio can remarkably influence the pH and the concentration of phosphate ions in the pore solution [21], the depassivation and corrosion behaviour of the reinforcing steel embedded in MKPC may also be affected. This is because, in PC-based cementitious materials, it has been reported that the corrosion resistance of steel to chloride-induced attack, which can be assessed by the critical chloride value, increases with increasing pH [22]. On the other hand, the phosphate ion, which is commonly reported to be an effective corrosion inhibitor in reinforced PC concrete [23], can adsorb to, or even precipitate in, the oxide film formed on the steel surface, inhibiting the pitting corrosion [24, 25]. However, the inhibition of phosphate ions is also affected by pH and chloride concentration. For example, it has been reported that in simulated PC pore solution the corrosion resistance of steel to chloride-induced attack usually increases with an increasing phosphate-to-chloride (P/Cl) molar ratio [26, 27], and it has even been claimed that above a critical P/Cl ratio the chloride-induced corrosion can be fully inhibited [27]. On the other hand, the critical P/Cl ratio is also influenced by the pH of electrolyte. For example, Mohagheghi *et al.* [27] reported that the critical P/Cl ratio is 5.5 when the pH is around 8.8, while Yohai *et al.* [28] showed that a P/Cl ratio of 1.0 is enough for the corrosion inhibition in PC with a pH of 13.0. Based on the above literature review, it is evident that the M/P could have some conflicting effects on the resistance of reinforcing steel to chloride-induced attack in MKPC systems, namely, when the M/P increases, the pH value will increase whilst the phosphate concentration will decrease; the former can increase the resistance to chloride-

induced attack, while the latter may generate a less favourable effect. On the other hand, when the M/P decreases, the opposite effects may occur. That is, the pH will decrease whilst the phosphate concentration will increase. In this case, the former can decrease the resistance to chloride-induced attack while the latter may benefit. It has been found by limited research that the resistance of reinforcing steel to chloride-induced attack in MPC systems is higher than what has been anticipated [17, 29, 30], which was attributed to the formation of iron phosphate and hydration products on the surface of mild steel embedded in MPC exposed to chloride ions [29]. However, the combined role of phosphate ions and pH played in the depassivation and corrosion of mild steel is still unclear. Furthermore, the critical chloride value for the depassivation of steel in MKPC system is also not available in the literature. Moreover, the effect of M/P ratio on the depassivation and corrosion of mild steel was not revealed and, to date, it is still largely unknown, even though this value is important for the mix design and service life prediction.

Therefore, a systematic study to investigate the effects that the M/P ratios may have on the depassivation and corrosion of mild steel in MKPC was carried out by the authors and the results are reported in this paper. The depassivation and corrosion behaviour of the mild steel in the pore solutions of MKPC formulated with different M/P ratios was assessed via open circuit potential (OCP), linear polarization resistance (LPR), electrochemical impedance spectroscopy (EIS) and potentiodynamic polarization. The chemical composition of the corrosion products formed in the MKPC pore solution was then analysed by X-ray Photoelectron Spectroscopy (XPS) and Raman spectroscopy. Based on the experimental results obtained in this study, the possible mechanisms of the chloride-induced depassivation and corrosion of mild steel in MKPC matrices are then proposed and discussed in this paper.

2 Experimental

2.1 Materials

The MKPC pastes were formulated with an industry grade dead burnt magnesia (DBM) supplied by Changyi New Materials Ltd. in Guangzhou, China and a reagent grade potassium dihydrogen phosphate (KH_2PO_4, KDP) from Prayphos^{TM} with a purity of 98%. Borax ($Na_2B_4O_7 \cdot 10H_2O$), which was employed as a retarder, was supplied by Sigma-Aldrich with a purity of more than 99.5%. A PC-based paste formulated with a CEM I Portland cement (PC) conforming to BS EN 197-1:2011 and supplied by Quinn Cement (Ireland) was also prepared as a control mix in this study. The chemical composition of the PC is shown in Table 1. Mild steel of Φ 16 mm, which is widely used as a reinforcing steel in concrete, was used to investigate the corrosion behaviour. The chemical composition of the mild steel is presented in Table 2. The mild steel was sectioned into small pellets with a thickness of 10 mm. Prior to the electrochemical tests, the pellet surfaces were polished using sandpapers of grit 100, 400, 800, 1200 and 3000 respectively and then cleaned with deionised water and acetone.

Table 1 Chemical composition of PC (wt%)

Oxide	SiO_2	Al_2O_3	Fe_2O_3	CaO	MgO	K_2O	Na_2O	SO_3
Content	23.00	6.15	2.95	61.30	1.80	0.68	0.22	2.50

Table 2 Chemical composition of mild steel (wt%)

Fe	C	P	S	Mn	Si	Cu
Bal.	0.170	0.005	0.017	0.460	0.260	0.019

2.2 Mix design

In this study, in order to investigate the influence of M/P ratio on the depassivation and corrosion behaviour of mild steel, MKPC pastes with M/P ratios of 7, 12 and 17 were formulated. It should be noted that same M/P ratios were also adopted in a previous paper for

the investigation of the effect of M/P ratios on the passivation of mild steel in MKPC [16]. A W/C ratio of 0.22 was fixed for all the MKPC mixes. In the case of MKPC, the term cement refers to the combination of MgO and KDP. In addition, Borax was added at 15% by the weight of MgO to adjust the setting time of MKPC. The MKPC mix formulations as well as the batch weights of the constituent materials employed in this study are presented in Table 3. To compare the performance of mild steel in the MKPC systems with that in PC, a PC paste with a W/C ratio of 0.45, which generated similar fluidity as those of the MKPC pastes, was employed in this study as a control.

Table 3 Mix design and batch weight of MKPC pastes

Mix proportion			**Batch quantity / g**			
M/P	Borax	W/C	MgO	KDP	Borax	Water
7	15%	0.22	674.60	325.40	101.19	220
12	15%	0.22	780.41	219.59	117.06	220
17	15%	0.22	834.30	165.70	125.14	220

2.3 Manufacture of the paste specimens

The mixing procedure adopted in this study involved dry-mixing the powders for one minute and then further mixing with water for three minutes in a vertical-axis planetary mixer. The fresh pastes were then cast in cylindrical polyethylene moulds (90 mm x Φ 35 mm) and cured at a constant temperature of 20 °C for 24 hours before being demoulded. After demoulding at 24 hours, the pastes were used for the pore solution extraction since preliminary trials indicated that 24-hour duration is the minimum time needed for the MKPC pastes to develop a relatively stable pore solution for the subsequent corrosion studies [31].

2.4 Pore solution extraction

A steel-die facility similar to that first described by Longuet [32, 33] and Barneyback and Diamond [34] was used for the extraction of MKPC and PC pore solutions. The same

procedure and apparatus as used in [16] were employed. During the extraction process, whilst sufficient pore solution can be collected, a pressure lower than 400 MPa was applied in this study. This is because when the applied pressure is higher than 400 MPa, there is an increase in the concentration of certain ions in the pore solution with the increase of the pressure applied, leading to the concerns over the reliability of this technique [35]. It should be noted that the surface of the paste used for the extraction should be wiped with a wet cloth in order to achieve the saturated and surface dry condition so that the influence of any extra water can be avoided. This is because the extra water may lead to a reduction in both the pH and ion concentrations of extracted pore solution. In addition, to minimise the possible carbonation of the extracted pore solutions by air, the extracted pore solutions were sealed in a centrifuge tube immediately after extraction. Prior to the subsequent pH, ion chromatograph (IC) and corrosion tests as described below, the extracted pore solution was filtered through a 0.45 μm filter paper in order to remove any tinny debris which might have been introduced during the extract process.

2.5 Test methods

2.5.1 Characterisation of the pH and chemical composition of the pore solution

The pH values of the MKPC and PC pore solutions were measured with a Thermo Scientific Orion 8165BNWP-ROSS Sure-Flow pH electrode. The pH electrode was put in the pore solution until a stabilized pH value was obtained.

The chemical compositions of the MKPC and PC pore solutions were analysed with a Dionex ICS 900 ion chromatograph (IC) analyser. The pore solutions were first diluted at various dilution factors, depending on the concentration of the solution, in order to meet the

requirement for the concentration limit of each ion. The diluted pore solutions were then analysed with an ionic chromatograph analyser.

2.5.2 Electrochemical tests

The following electrochemical tests were carried out to obtain the thermodynamic and kinetic information on the passivation and corrosion behaviours of mild steel.

- Open circuit potential (OCP) and linear polarisation resistance (LPR), which are commonly used to determine the critical chloride value, were used to identify the critical chloride value for the depassivation of the mild steel in the MKPC and PC pore solutions [36].
- Electrochemical impedance spectroscopy (EIS) was used to acquire more detailed kinetic parameters of corrosion in addition to those obtained from LPR measurements, including the resistance of oxide film and the charge transfer resistance.
- Potentiodynamic polarisation was adopted to obtain the information on the separate anodic and cathodic corrosion processes as well as more detailed electrochemical parameters, such as corrosion potential, pitting potential, corrosion current density, and oxide current density.

A tailor-designed cell with a three-electrode configuration as employed in a previous work [16] was used in this study to conduct the electrochemical tests, as shown in Fig. 1. The detailed description of the setup for the electrochemical tests can be found in [16].

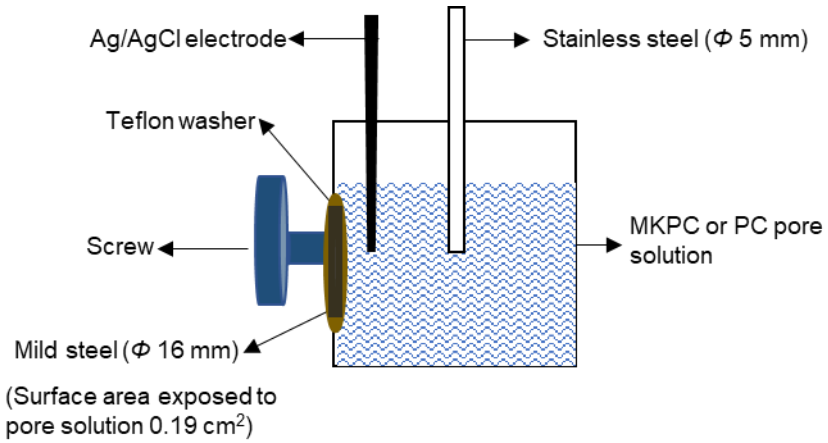

Fig. 1. Schematic diagram of the test setup for electrochemical measurements (adapted from [16])

The mild steel pellets were inserted into the side wall of the cell immediately after polishing, followed by filling the extracted MKPC or PC pore solutions into the cell. The mild steel pellets were then stabilized in the cell for 15 mins before carrying out various electrochemical tests by connecting the three electrodes in the cell to a “Gill AC” potentiostat (ACM Instruments UK). All the electrochemical tests were performed at a constant temperature of 20 °C. In this study, the LPR measurements were carried out from -15 mV_{OCP} to 15 mV_{OCP} with a scan rate of 0.16 mV/s. The EIS tests were performed using an applied AC signal amplitude of 32 mV RMS which ensures the linearity and the stability of EIS data. The frequency of EIS was ranged from 100 kHz to 0.01 Hz. The obtained EIS data were fit by ZSimpWin software. The potentiodynamic polarisation was carried out from -0.8 V_{OCP} to 1.0 $V_{Ag/AgCl}$ with a scan rate of 0.16 mV/s.

In order to simulate the potential application of reinforced MKPC concrete in marine environment, prior to the corrosion process, a passivation process was firstly performed for the mild steel as follows. Immediately after polishing, the mild steels were exposed to the pore solutions and the OCP measurements were carried out at 15 minutes, 24, 72 and 168 hours

to monitor the passivation behaviour of mild steel. Once the mild steel was confirmed to be passivated, 0.05 M NaCl was added into the pore solution every 24 hours. The corresponding OCP, LPR and EIS tests were undertaken 24 hours after the addition of NaCl at each interval to identify the critical chloride values needed for the depassivation of mild steel in each pore solution. In addition, another passivated mild steel was prepared to conduct the potentiodynamic polarisation test by adding 0.6 M chloride ions in the pore solution. The 0.6 M chloride concentration was used in the potentiodynamic polarisation tests to simulate the marine environment.

2.5.3 Micro-scale techniques

2.5.3.1 Scanning electron microscopy (SEM) / Energy-dispersive X-ray spectroscopy (EDS)

After being exposed to MKPC or PC pore solutions with a chloride concentration of 1.4 M, the mild steel was cleaned in an ultrasonic bath and then dried to remove the species originated from the pore solutions. The morphology of the corroded steel surface was then characterised under SEM (Carl Zeiss XB1540 “Cross-Beam” focused-ion-beam microscope). EDS was also carried out to identify the composition of the products formed on the steel surface.

2.5.3.2 XPS

The composition of the corrosion products formed on the surface of mild steel were also characterised with XPS after being exposed to MKPC or PC pore solutions with a chloride concentration of 1.4 M. A ESCALAB250Xi Thermo Scientific K-alpha photoelectron spectrometer with Al Kα (1486.6 eV) as X-ray source and an analytical chamber with a base pressure of 10^{-6} Pa were used to collect XPS spectra. The diameter of the analysed area was 800 μm. The high-energy resolution spectra were collected for oxygen (O 1s), carbon (C 1s), iron (Fe 2p), and phosphate (P 2p) elements. The high-resolution XPS spectra were then

265 analysed using the CasaXPS software and C 1s peak (284.6 eV) was used for the calibration
266 of the measured XPS spectra. The fitting procedures of XPS spectra involved a Shirley
267 background and deconvolution by an asymmetric Gaussian-Lorentzian sum function.

268

269 *2.5.3.3 Raman spectroscopy*

270 After XPS analyses, Raman spectroscopy measurements were carried out to complement the
271 EDS obtained from SEM to further characterise the composition of the corrosion products
272 formed on the mild steel. A Renishaw 2000 micro-Raman spectrometer was used to obtain
273 the *Ex-situ* Raman spectra in the surface region of mild steel. A sensitive CCD detector was
274 coupled to the microscope for point-by-point analyses. Leica 50× (NA = 0.50) lens was used,
275 through which the laser with a wavelength of 514.5 nm and a spot size of 1.4 μm in diameter
276 was focused on the specimens. It should be noticed that the laser power adopted in this study
277 was only 0.73 mW. This low laser power was purposely adopted to reduce the heat generated
278 during the Raman analysis in order to avoid the change to the composition of corrosion
279 products under high temperature [37]. The exposure time for the spectra recording was 60
280 seconds with 5 accumulations, which can improve the signal-to-noise ratio.

281

282 3 Results and discussion

283 3.1 pH and phosphate concentration of the MKPC pore solutions

284 To understand the effect that pH and phosphate concentration of the MKPC may have on the
285 depassivation and corrosion of mild steel in different MKPC matrices, the compositions of the
286 extracted MKPC and PC pore solutions were characterised and the results are shown in Table
287 4. The presence of small amounts of sulfate and chloride ions could be attributed to the
288 impurities existing in the raw materials used in this study. Most importantly, it can be noticed

289 that the hydrogen-phosphate (HPO_4^{2-})/phosphate (PO_4^{3-}) ions, which was originated from one
290 of the raw materials, KH_2PO_4, dominates the pore solution chemistry of MKPC systems. It
291 should be highlighted that these anions (HPO_4^{2-}/PO_4^{3-}, SO_4^{2-} and Cl^-) are believed to compete
292 with each other in adsorbing onto the surface of steel [38]. However, the HPO_4^{2-}/PO_4^{3-} ions
293 was reported to have a higher adsorption capability than SO_4^{2-} and Cl^- ions [39]. Thus, the
294 presence of small amounts of SO_4^{2-} and Cl^- ions in the MKPC pore solutions would have a
295 marginal effect on the corrosion inhibition role to be played by HPO_4^{2-}/PO_4^{3-} ions (as discussed
296 in Section 3.7 below).

297 Moreover, it can be noted that the concentration of HPO_4^{2-}/PO_4^{3-} ions significantly increased
298 with decreasing M/P ratio, with the phosphate concentration of M/P 7 being three orders of
299 magnitude higher than that of M/P 17. On the contrary, the pH of the pore solution of M/P 7
300 (pH 8.69) is much lower than those of M/Ps 12 (pH 10.21) and 17 (pH 10.87). Overall, the pHs
301 of the MKPC pore solutions are significantly lower than that of the PC (pH 12.89). It should be
302 noted that, to clearly distinguish HPO_4^{2-} and PO_4^{3-} ions by existing analytical techniques, such
303 as IC, Raman spectroscopy, XPS, has proven to be difficult [26, 40, 41]. The reason for this
304 could be due to the similarity in the chemical structures between HPO_4^{2-} and PO_4^{3-} ions.
305 However, based on the thermodynamics of phosphate species, HPO_4^{2-} rather than PO_4^{3-} could
306 probably be the dominant specie in the MKPC pore solutions with pH values ranging from 8.69
307 to 10.87 [42]. Nevertheless, the kinetic process occurring in the MKPC pore solutions could
308 be non-equilibrium and thus HPO_4^{2-} and PO_4^{3-} could possibly coexist. In order to accurately
309 represent the possible phosphate species existing in the MKPC pore solutions, the phosphate
310 species in the MKPC pore solutions in this study are denoted as HPO_4^{2-}/PO_4^{3-}, even though
311 in most cement literature the phosphate species in the MKPC pore solutions have usually
312 been simplified as PO_4^{3-} ions [43, 44].

313

314

315 Table 4 Chemical composition and pH of the extracted MKPC and PC pore solutions

	Hydrogen-phosphate /Phosphate (mg/l)	Sulphate (mg/l)	Chloride (mg/l)	Solution pH
M/P 7	153297.37	564.19	54.35	8.69
M/P 12	28472.34	513.53	104.16	10.21
M/P 17	658.18	606.08	112.18	10.87
PC	/	656.37	619.42	12.89

316

317 3.2 Corrosion potential E_{corr} and corrosion resistance R_p

318 3.2.1 Passivation behaviour

319 Fig. 2 shows the evolution of the E_{corr} of mild steel over immersion time in the chloride-free
320 MKPC or PC pore solutions. As can be seen, the E_{corr} values increased significantly during
321 the first 24 hours. However, the increasing rate of the E_{corr} values was much slower afterwards
322 and remained above -200 $mV_{Ag/AgCl}$ at the age of 168 hours. This suggests that the mild steel
323 was rapidly passivated in the MKPC pore solutions during the first 24 hours, and finally a
324 compact oxide film was formed at the age of 168 hours [45]. The PC specimen also exhibits
325 a similar trend of the E_{corr} over immersion time to those of the MKPC specimens, which is
326 consistent with the previous studies in the literature, indicating a protective oxide film was also
327 formed on the mild steel in PC [46]. Thus, based on the results shown in Fig. 2, all the mild
328 steel specimens were immersed in the chloride-free MKPC or PC pore solutions for 168 hours
329 to ensure that a compact passive film was formed before they were exposed to chloride ions
330 in the depassivation tests.

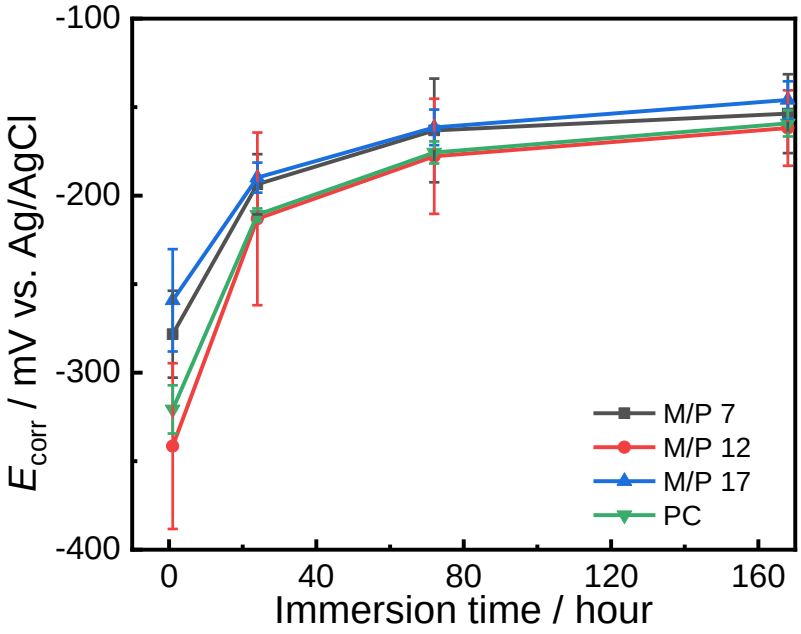

Fig. 2. Evolution of the E_{corr} of mild steel over immersion time in the MKPC and PC pore solutions

3.2.2 Critical chloride value

To obtain the critical chloride value, the passivated mild steel was exposed to chloride ions at incremental concentrations in the MKPC and PC pore solutions and the depassivation and corrosion behaviour was then characterised by electrochemical techniques. The chloride-induced corrosion of mild steel occurs when the corrosion resistance R_p obtained from the LPR test and the corrosion potential E_{corr} obtained from the OCP measurement decrease suddenly and show a clear turning point [47]. The corresponding chloride concentration is then considered as the critical chloride value for the initiation of the depassivation and corrosion of mild steel. Thus, the critical chloride value is critical to the assessment of the corrosion resistance of mild steel in MKPC pore solutions.

The evolution of the E_{corr} and R_p of the mild steels over chloride concentrations in the MKPC pore solutions are shown in Figs. 3(a) and (b), respectively. It can be observed that the E_{corr}

and R_p values of all the specimens remain high and stable when the chloride concentration was below certain levels, namely, $[Cl^-]$<0.40 M for M/P 7, $[Cl^-]$<1.00 M for M/P 12, $[Cl^-]$<1.35 M for M/P 17 and $[Cl^-]$<0.04 M for PC specimen. This indicates that the mild steel remains passivated below these chloride concentrations, respectively. In addition, it can be noted that the R_p values show an increasing trend with increasing M/P ratios before a certain chloride concentration is reached, indicating that the passivity of the mild steel increases with M/P ratios. However, the R_p values of the M/Ps 12 and 17 samples dropped dramatically to below 260 kΩ·cm^2, when the chloride concentrations of 1.00 M and 1.35 M were reached for M/Ps 12 and 17 specimens, respectively. It should be noted that 260 kΩ·cm^2 has been determined as a critical R_p value for the depassivation and the occurrence of chloride-induced corrosion of steel in PC systems [48]. As the R_p values of M/P 7 specimen are lower than 260 kΩ·cm^2 at all the chloride concentrations, it seems that no protective film was formed on the surface of the mild steel in the M/P 7 pore solution. However, as the cement chemistry of MKPC is so different from that of PC, the values of the Tafel constant B of the MKPC and PC systems could be different. This may result in different critical R_p values for the passivation and depassivation of mild steel in the MKPC pore solutions. Therefore, it is considered inappropriate to judge the critical chloride value based on a fixed R_p value. Instead, the chloride concentration corresponding to the turning point at which the R_p and E_{corr} starts to reduce should be considered as the critical chloride value. However, it should be noted that the presence of phosphate ions could lead to a lower activity coefficient of chloride ions and thus the effective chloride concentration might be lower than the identified chloride threshold values shown in Fig. 3 [49]. Nevertheless, regardless of the effect of the other ions (and hence the activity coefficient), the unique pore solution chemistry of MKPC (as compared to PC) is indeed its strength, and thus, the benefits which can be obtained by using MKPC to replace PC to manufacture reinforced concrete in practice. Therefore, in terms of engineering practice, the measured threshold chloride values [47, 50] as presented in Table 5 is considered to be more relevant for the design and service life prediction purposes of MKPC concrete.

It can be seen that the critical chloride concentration increases with M/P ratio, which is consistent with the increasing trend of R_p vs. M/P ratio. Therefore, the increased critical chloride concentration as shown in Table 5 could be attributed to the improved quality of the oxide film formed in the MKPC with increasing M/P ratio, leading to an increase in its resistance to the chloride-induced attack. It is worth noticing that the critical chloride value of the mild steel in the PC pore solution is only 0.02 M~0.04 M, which is consistent with the critical chloride value reported in the literature [51]. It is evident that the critical chloride values of the mild steels in the MKPC pore solutions are more than one order of magnitude higher than that in the PC pore solution, which demonstrates that the corrosion resistance of mild steel to chloride-induced attack is much enhanced in MKPC. Moreover, the mild steels in the MKPC pore solutions exhibit higher R_p values than that in PC specimen even when the chloride concentration exceeds the critical chloride values. This could be related to the pore solution chemistry of MKPC, in particular the HPO_4^{2-}/PO_4^{3-} ions, which can interact with the mild steel during the corrosion process, leading to an increased resistance (as will be further discussed below).

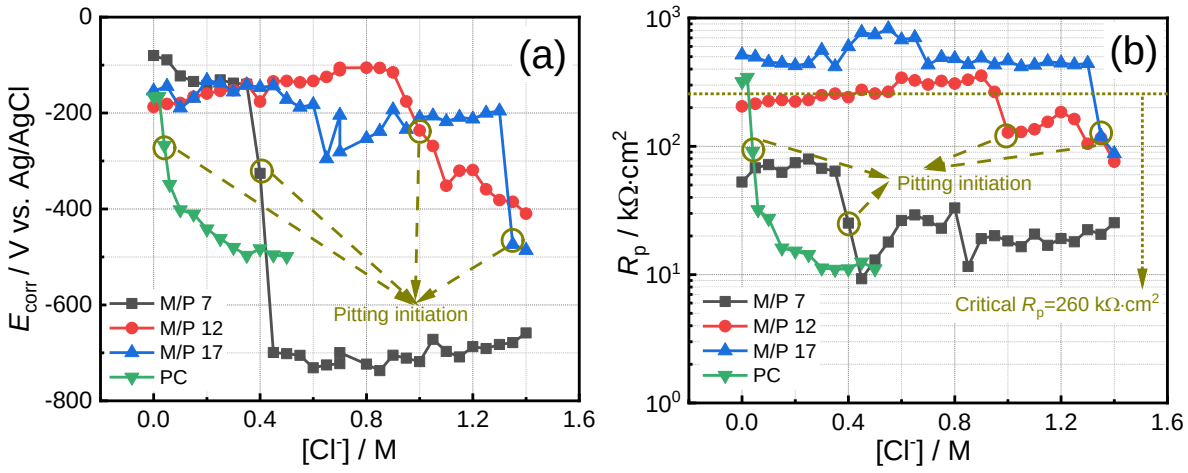

Fig. 3. (a) E_{corr} and (b) R_p evolution of the mild steel with increasing chloride concentrations in the MKPC and PC pore solutions (Note: the chloride concentration was adjusted stepwise by 0.05 M NaCl every 24 hours)

396 Table 5 Identified critical chloride values for the mild steel in the MKPC and PC pore
397 solutions

Specimen	M/P 7	M/P 12	M/P 17	PC
$[Cl^-]_{crit}$ (M)	0.40	1.00	1.35	0.04

398

399

400 3.3 Electrochemical impedance spectrum

401 The depassivation and corrosion processes of the passivated mild steel in the MKPC pore
402 solutions at various chloride concentrations are also characterised by EIS and the data are
403 plotted in Fig. 4. Both the Nyquist plots (Figs. 4(a-1), (b-1) and (c-1)) and Bode plots (Figs.
404 4(a-2), (b-2) and (c-2)) are presented. It can be noted from the Nyquist plots (Figs. 4(a-1) and
405 (b-1)) that the diameters of the depressed capacitive semi-circle became much smaller when
406 the critical chloride values $[Cl^-]_{crit}$ were reached, respectively, for the mild steel samples in
407 different MKPC pore solutions, indicating a dramatic reduction in the resistance of the mild
408 steel to chloride-induced corrosion in the MKPC and PC pore solutions. In addition, it can be
409 observed from Fig. 4(b-1) that a semi-circle of small diameter appeared (as indicated by a
410 small circle with dashed line) in the low frequency range of the Nyquist plot of M/P 7 specimen.
411 This could be attributed to the fast change occurred at the surface of the mild steel in M/P 7
412 during the initial corrosion period, which can be measured during the EIS test in the low
413 frequency range [52]. However, as the concentration of chloride ions increased to 1.4 M, the
414 semi-circle of this small diameter in the low frequency range of the Nyquist plot of M/P 7
415 specimen disappeared (shown in Fig. 4(c-1)). This possibly indicates that the corrosion
416 reaction rate at the surface of the mild steel in the M/P 7 pore solution is reduced when the
417 chloride concentration was increased from critical level to 1.4 M, resulting in a stable state
418 reached on the steel surface during the EIS test.

419

Moreover, as can be noted from Figs. 4(b-2) and (c-2), the phase degrees in the middle frequency range of the Bode plot of M/P 7 specimen at the concentrations of $[Cl^-]_{crit}$ and $[Cl^-]$=1.4 M are higher than those of M/Ps 12 and 17 specimens. This implies that the capacitive behaviour of the oxide film formed on the surface of M/P 7 specimen is different from those on M/Ps 12 and 17 specimens, which could be attributed to a quite different composition of the oxide film formed on the surface of the mild steel in the M/P 7 pore solution (as further discussed in Section 3.7).

In order to quantitatively analyse the kinetics of the corrosion process, equivalent circuit is adopted to fit the EIS data. It can be observed from the Bode plots, as shown in Figs. 4(b-2) and (c-2), that two Bode phase peaks can be clearly observed for M/Ps 7 and 17 specimens which suggests that two time-constants should be included in the system. In addition, an inductive loop was identified in the Nyquist plot for M/P 7 specimen at $[Cl^-]_{crit}$ which suggests that an inductive element should also be included in the equivalent circuit for M/P 7 specimen (as shown in Fig. 5(b)). On the other hand, three Bode phase peaks can be observed in the Bode plots for M/Ps 12 specimen at $[Cl^-]_{crit}$ and $[Cl^-]$=1.4 M. Therefore, three time-constants are considered to be more appropriate (as shown in Fig. 5(c)). Additionally, one broad and high Bode phase peak is visible in the Bode plots of the passivated mild steel in all pore solutions as shown in Fig. 4(a-2). This could also be associated with two time-constants which might overlap with each other [53]. Thus, the equivalent circuit with two time-constants, as shown in Fig. 5(a), was adopted to fit the EIS data in Fig. 4 except those for M/P 7 at $[Cl^-]_{crit}$, M/P 12 at $[Cl^-]_{crit}$ and $[Cl^-]$=1.4 M. all these equivalent circuits show good fitting with much low chi-squared values (10^{-3}~10^{-4}). It should be noted that, in these equivalent circuit, R_s represents the resistance of the pore solution, R_f and Q_f stand for the resistance and capacitance of the layer formed on the surface of mild steel, respectively. In addition, R_{ct} and Q_{dl} are the charge transfer resistance and double layer capacitance, respectively, whilst L represents the inductance related to the adsorption process occurring on the surface of mild

steel [54, 55]. Additionally, the R_{ad} and Q_{ad} are the resistance and capacitance of the adsorption layer on the surface region respectively [56]. It is worth highlighting that both the Q_f and Q_{dl} are Constant Phase Element (CPE), since the passive film and the double layer on the mild steel is inhomogeneous [57]. The CPE can be expressed as follows [58]:

$$Z_{CPE} = [Q(jw)^n]^{-1} \quad \text{Eq. 2}$$

where Q is a capacitive constant with a unit of $\Omega^{-1}\cdot cm^{-2}\cdot s^n$, while n a constant power, with $-1 < n < 1$.

The EIS fitting results are further tabulated in Table 6. It can be found that the R_f and R_{ct} values of all the mild steel in the chloride-free MKPC pore solutions are significantly higher than those in the chloride-free PC pore solution. This indicates that the protective oxide films formed on the surface of mild steel in the MKPC pore solutions are more compact than that in the PC pore solution. Additionally, the R_{ct} values increase with the increasing M/P ratios in the chloride-free MKPC pore solutions, suggesting an increase in the protective capacity of the oxide film.

However, when the critical chloride concentrations were reached, all the specimens exhibited remarkable reduction in R_f and R_{ct} values in comparison to those in the chloride-free MKPC and PC pore solutions. This indicates that the steel/film interface could have been damaged due to the formation of chloride-induced pitting. On the other hand, when the chloride concentration is equal to the critical chloride concentration, the R_f and R_{ct} values increased with increasing M/P ratios. It should be highlighted that the R_f and R_{ct} values of M/P 7 specimen were lower than those of PC specimen, indicating that the M/P 7 specimen has the lowest

corrosion resistance. This could be related to the nature of the oxide film formed in M/P 7. It can be noticed that, even though the values of M/P 7 specimen are lower than those of M/Ps 12 and 17 specimens at the critical chloride concentration, the Q_f value of M/P 7 specimen is lower than those of M/Ps 12 and 17 specimens, and the corresponding n_f value of M/P 7 specimen is higher than those of M/Ps 12 and 17 specimens. This can be attributed to a different composition of the oxide film formed in M/P 7 when compared to those in M/Ps 12 and 17 [26]. This will be discussed in detail below. Nevertheless, further increasing the chloride concentration up to 1.4 M resulted in the increased R_f and R_{ct} values of M/P 7 specimen, indicating that the corrosion resistance of M/P 7 specimen increased. Similar results have been reported in the literature and this phenomenon has been attributed to the interaction between the phosphate ions and the dissolved iron ions [26]. It is worth noticing that when the M/P is low, the phosphate content becomes higher in the MKPC system which could explain the possible interaction between the phosphate and the dissolved iron as highlighted above. In contrast, the R_{ct} values of M/Ps 12 and 17 specimens decreased with the increased chloride concentration up to 1.4 M, which is consistent with the previous literature showing that corrosion resistance is decreased with the increasing concentration of chloride ion [36]. This could be explained by the intensified chloride attack to the mild steel with the increased chloride concentration. Nevertheless, the R_f and R_{ct} values increase with the increase of M/P ratio when the chloride concentration is equal to 1.4 M, which suggests that the corrosion resistance of mild steel increase with increasing M/P ratio during the corrosion process. Furthermore, it can be noted that the R_f and R_{ct} values of PC specimen are remarkedly reduced with the increased chloride concentration up to 1.4 M, which are significantly lower than those of MKPC specimens. This implies that compared to PC, MKPC can provide a better protection to reinforcing steel.

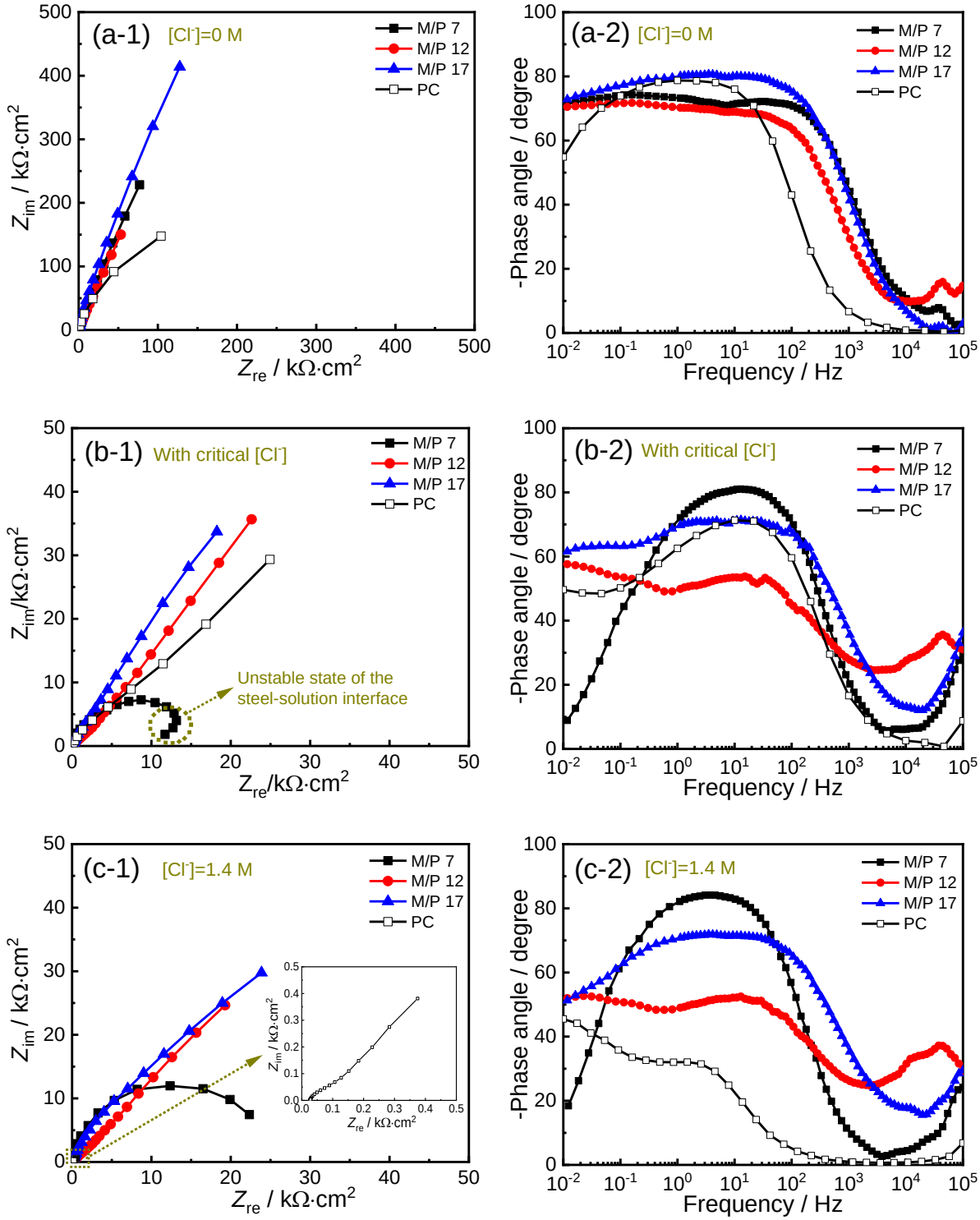

Fig. 4. EIS results of the mild steel in the MKPC and PC pore solutions: (a-1) Nyquist plot without addition of Cl^-; (a-2) Bode plot without addition of Cl^-; (b-1) Nyquist plot with addition of $[Cl^-]crit$; (b-2) Bode plot with addition of $[Cl^-]_{crit}$; (c-1) Nyquist plot with addition of 1.4 M Cl^-; and (c-2) Bode plot with addition of 1.4 M Cl^-

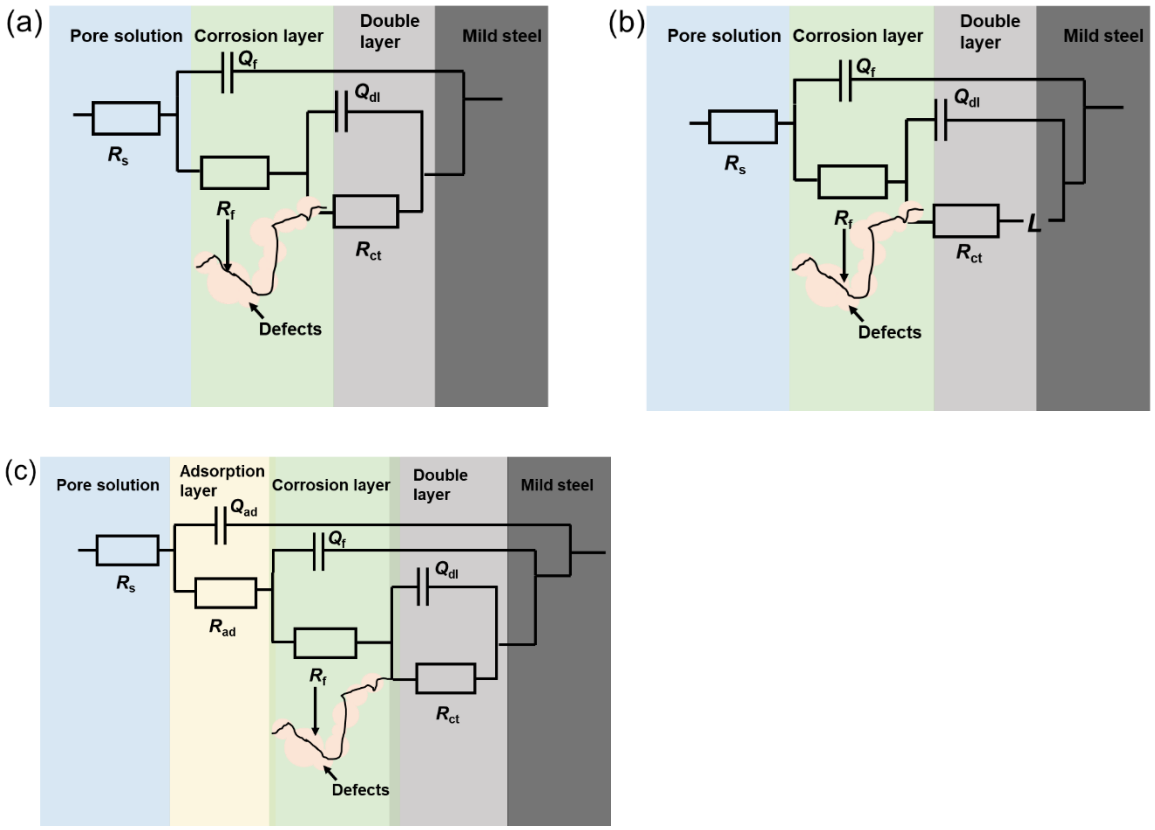

505 Fig. 5. Equivalent circuit for the fitting of the EIS data obtained in this study: (a) *R(QR(QR))*;

506 (b) *R(QR(Q(RL)))*; and (c) *R(Q(R(Q(R(QR)))))*.

Table 6 The fitted electrochemical parameters for impedance spectra of the mild steel in the MKPC and PC pore solutions

	Specimen	R_s / kΩ·cm^2	R_a / kΩ·cm^2	Q_a / μΩ^{-1}·cm^{-2}·s^n	n_a	Q_f / μΩ^{-1}·cm^{-2}·s^n	n_f	R_f / kΩ·cm^2	Q_{dl} / μΩ^{-1}·cm^{-2}·s^n	n_{dl}	R_{ct} / kΩ·cm^2	chi squared value
[Cl$^-$]=0 M	M/P 7	14.87	/	/	/	21.86	0.89	2.57	13.82	0.76	2520.00	3.46 x 10^{-4}
	M/P 12	23.38	/	/	/	47.12	0.80	76.43	3.43	0.87	6081.00	1.12 x 10^{-3}
	M/P 17	15.47	/	/	/	20.51	0.91	92.59	1.77	0.51	8548.00	5.08 x 10^{-4}
	PC	49.24	/	/	/	38.94	0.96	1.27	17.29	0.74	433.36	1.08 x 10^{-3}
[Cl$^-$]=[Cl$^-$]$_{crit}$	M/P 7	7.47	/	/	/	69.26	0.82	0.69	39.42	0.68	6.45	8.32 x 10^{-3}
	M/P 12	8.80	75.25	28.89	0.58	41.82	0.71	12.48	47.71	0.83	203.70	2.31 x 10^{-3}
	M/P 17	5.69	/	/	/	129.40	0.82	25.00	95.67	0.83	310.40	9.43 x 10^{-4}
	PC	27.71	/	/	/	33.59	0.95	1.08	80.48	0.60	68.07	5.43 x 10^{-4}
[Cl$^-$]=1.4 M	M/P 7	9.26	/	/	/	114.10	0.97	0.65	18.61	0.37	30.50	2.11 x 10^{-3}
	M/P 12	8.81	42.99	2.21	0.83	156.40	0.62	3.55	222.00	0.76	126.30	1.36 x 10^{-3}
	M/P 17	6.00	/	/	/	131.10	0.82	29.90	81.99	0.63	184.10	2.35 x 10^{-3}
	PC	25.71	/	/	/	5586.00	0.57	0.52	11280	0.88	6.02	5.05 x 10^{-3}

3.4 Potentiodynamic polarisation

Fig. 6 displays the potentiodynamic polarisation curves of the passivated mild steel in the MKPC and PC pore solutions with 0.6 M chloride ions. The 0.6 M chloride concentration was employed to simulate the salinity of the seawater so that the properties of the passive film formed in MKPC could be assessed under an environment similar to that to be faced in practice. Fig. 6(a) shows the cathodic, active, transition, passivity and transpassivity regions of a typical potentiodynamic polarisation curve (as obtained from the mild steel in the M/P 17 pore solution). The potentiodynamic polarisation curves of MKPC and PC specimens are then compared in Fig. 6(b). It can be observed from Fig. 6(b) that the polarisation curves of the mild steels in the MKPC pore solutions have obvious passivity regions, while this is difficult to be recognised in the PC pore solution. This implies that the oxide films formed on the surface of the mild steels in the MKPC pore solutions are more resistant to the chloride-induced attack in comparison to that formed in PC. Moreover, the polarisation curves of the mild steels in the MKPC pore solutions exhibit the active region and transition region, These regions are absent from the potentiodynamic polarisation curve of the mild steel in PC, which is consistent with the previous study [59]. This could be related to the dissolution of iron and the re-precipitation of iron hydroxide/oxide or iron phosphate on the surface of the mild steels in MKPC [60]. In contrast, the iron could continuously dissolve from the steel substrate in PC due to the absence of HPO_4^{2-}/PO_4^{3-} ions. Furthermore, a second current peak appears in the polarisation curves of MKPC specimens, in particular, the second peak for M/P 7 specimen is the highest. This could be ascribed to the further anodic dissolution of iron due to the chloride-induced attack at high potential, followed by the precipitation of insoluble iron phosphates [61].

The electrochemical parameters, including corrosion potential E'_{corr}, pitting potential E_{pit}, corrosion current density i_{corr}, and oxide current density i_{pass}, obtained from Fig. 6 are summarized in Table 7. As can be seen that, both the i_{corr} and i_{pass} values of the MKPC specimens are lower than those of PC specimen, which indicates that the oxide film formed

on the surface of the mild steel in MKPC is more protective and resistant to the chloride-induced attack than that in PC. This is consistent with the results of the critical chloride values presented in Section 3.2.2. Moreover, both the i_{corr} and i_{pass} values decrease with the increased M/P ratio, suggesting that the increasing M/P ratio contributes to an increased corrosion resistance of mild steel. On the other hand, the E'_{corr} values of the MKPC specimens are lower than that of PC specimen, which is inconsistent with the E_{corr} results mentioned in Section 3.2.2. The lower E'_{corr} values of the MKPC specimens in the polarisation curves could be due to the inhibition role played by the HPO_4^{2-}/PO_4^{3-} ions in the MKPC pore solutions. It has been known that the anodic inhibition can lead to an enhancement of E'_{corr} [62], while the anodic-and-cathodic-mixed inhibition results in a slight change in the E'_{corr} value [63]. It must be noted that due to the lower E'_{corr} values of the MKPC specimens than that of the PC specimen, the cathodic potentials of the MKPC specimens fall into in the ranges of hydrogen evolution reaction [64]. In contrast, the main reaction occurring at cathodic potentials of the PC specimen is dominated by oxygen reduction reaction due to the much higher E'_{corr} of the PC specimen, which is consistent with those reported in the literature [65]. Therefore, based on the results presented in Fig. 6, it could be deduced that, different from the steel corrosion in PC system, a change in the oxygen content might not influence the corrosion process of steel in MKPC. Nonetheless, further investigation is still needed to verify this hypothesis. In addition, as has been well established, the potential differences, ΔE, between E_{pit} and E'_{corr} can be used as a criteria to assess the corrosion susceptibility of steel [66, 67]. As listed in Table 7, ΔE ($\Delta E = E_{pit} - E'_{corr}$) of the MKPC specimens are significantly higher than that of PC specimen, indicating that the chloride-induced corrosion resistance of the oxide film formed in MKPC is markedly higher than that in PC.

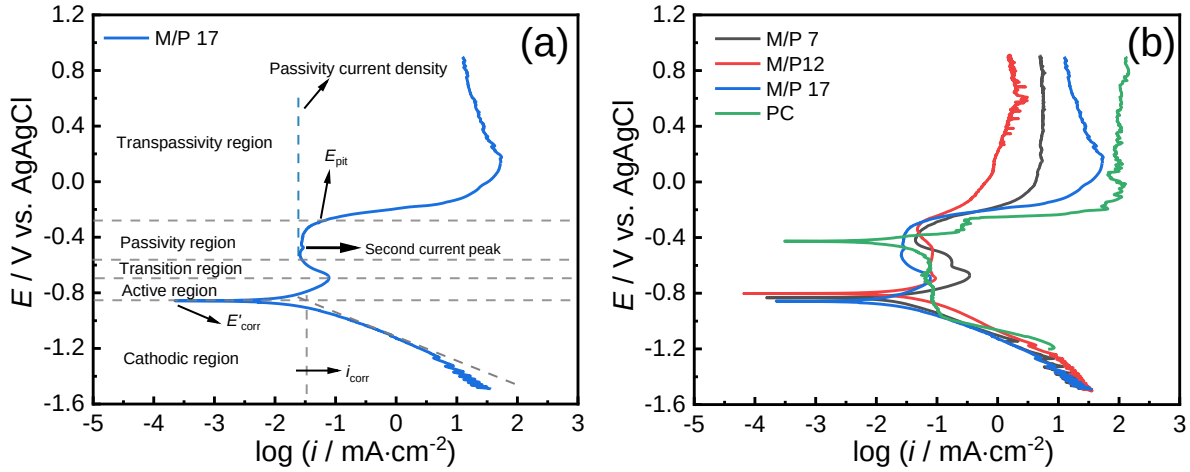

Fig. 6. (a) Illustration of various regions in a typical potentiodynamic polarisation curve; and (b) potentiodynamic polarisation curves of the passivated mild steel in the MKPC and PC pore solutions with the addition of [Cl^-]=0.6 M.

Table 7 Typical parameters obtained from the potentiodynamic polarisation curves of the passivated mild steel in the MKPC pore solutions with 0.6 M chloride ions

Specimen	E'_{corr} (mV)	E_{pit} (mV)	ΔE (mV)	i_{corr} (μA/cm^2)	i_{pass} (μA/cm^2)
M/P 7	-824.74	-297.60	527.14	39.23	145.21
M/P 12	-798.32	-294.30	504.02	39.67	82.41
M/P 17	-851.35	-289.90	561.45	34.68	26.31
PC	-421.09	-292.31	128.78	41.73	321.36

3.5 Morphology of the corrosion products

The morphology of the surface of the mild steels in the MKPC pore solutions after adding 1.4 M chloride ions is shown in Fig. 7. It must be noted that the 1.4 M chloride concentration was employed to ensure that corrosion would occur on the mild steels immersed in all the MKPC pore solutions according to the results shown in Table 5. It can be observed in Fig. 7 that porous corrosion products are present on the surface of the mild steels immersed in all the MKPC pore solutions and the amount of corrosion products decreased with the increase of M/P ratio. In comparison, the PC specimen exhibit a much rougher surface with large amounts of porous corrosion products compared to MKPC specimens. This indicates that the mild steel

in the PC pore solution suffered more severe damage from the chloride-induced corrosion than that in MKPC, which is consistent with the electrochemical results reported above.

EDS was employed to identify the composition of the corrosion products formed on the surface of the mild steel in the MKPC and PC pore solutions and the element composition is shown in Table 8. The existence of Fe and O elements in all the specimens implies that the porous products on the surface of mild steel is the corrosion products which are composed of iron hydroxide/oxide. On the other hand, the presence of P element in the corrosion products of M/Ps 7 and 12 specimens could be attributed to the formation of iron phosphate as one of the corrosion products, or the incorporation of the main hydration products, k-struvite ($MgKPO_4 \cdot 6H_2O$), into the corrosion products. However, the ratios of Mg/P and K/P in the corrosion products of the M/Ps 7 and 12 specimens are less than those in the MKPC hydration products such as $MgKPO_4 \cdot 6H_2O$. Thus, it could be deduced that iron phosphate might have been formed in the corrosion products of M/Ps 7 and 12 specimens. In addition, since the P/O ratios of the corrosion products formed in M/Ps 7 and 12 specimens are less than that of HPO_4^{2-}/PO_4^{3-} ion, it can also be deduced that, not only the iron phosphate, but the iron hydroxides/ oxides could also exist in the corrosion products of M/Ps 7 and 12 specimens. Interestingly, there is little P element identified in the corrosion products of M/P 17 specimen, which indicates that the main corrosion products in M/P 17 could be iron hydroxides or oxides. However, based on the EDS results alone, it cannot clearly identify the corrosion products formed. Therefore, the corrosion products were further characterised by XPS and Raman spectroscopy as reported in detail below.

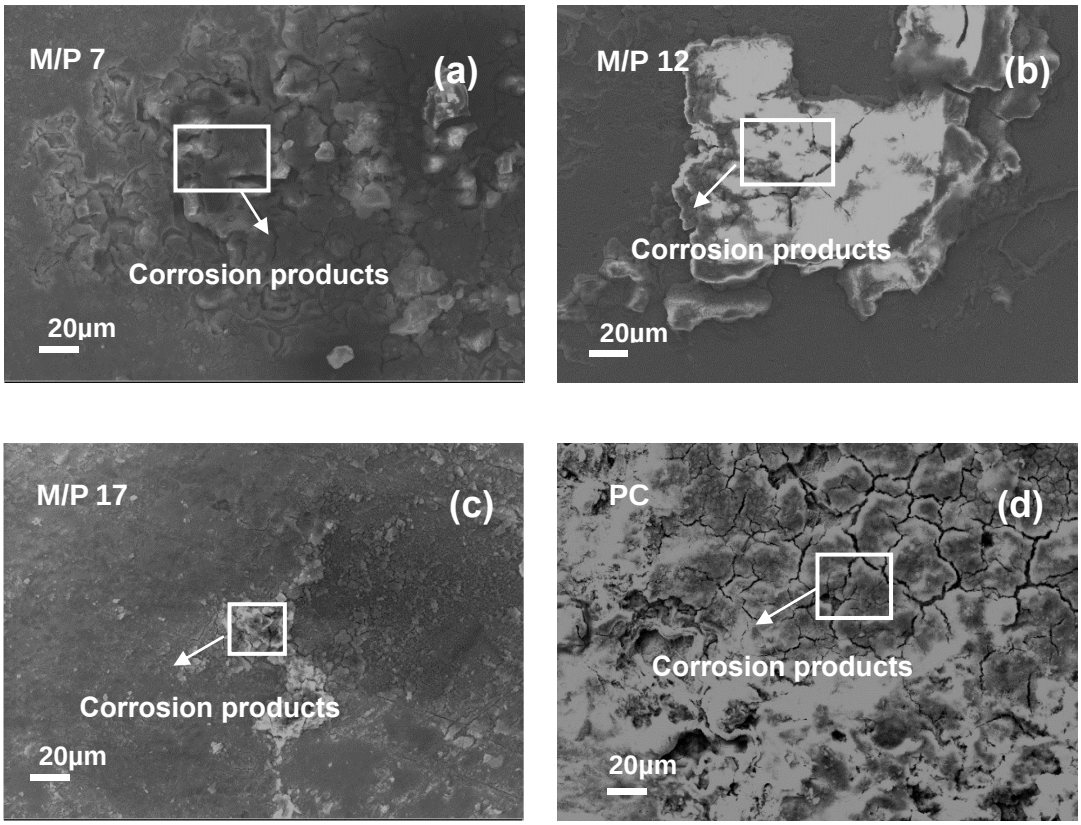

Fig. 7. SEM images of the surface of the mild steels immersed in the MKPC and PC pore solutions after adding 1.4 M chloride ions: (a) M/P 7; (b) M/P 12; (c) M/P 17; and (d) PC

Table 8 The elements of the corrosion products obtained from EDS (at.%)

	Fe	O	P	Mg	K	Cl
M/P 7	16.05	34.37	4.24	0.85	2.22	0.26
M/P 12	27.89	20.13	2.24	0.50	1.06	0.53
M/P 17	23.08	34.32	0.35	0.00	0.21	0.95
PC	17.32	33.33	/	/	/	0.74

3.6 Composition of the corrosion products

3.6.1 XPS

In order to clearly identify the composition of the corrosion products formed on the surface of mild steel in the MKPC pore solutions after adding 1.4 M chloride ions, the XPS was conducted and the high resolution spectra of Fe $2p_{3/2}$, O 1s and P 2p are shown in Fig. 8. As can be seen,

the deconvolution of Fe $2p_{3/2}$ spectra exhibits peaks at 706.6, 709.8 and 711.2 eV which can be attributed to Fe^0, Fe^{2+} and Fe^{3+}, respectively [68, 69]. Additionally, the peaks at 529.5 eV and 531.2 eV in the O spectra can be assigned to the binding energies of the O^{2-} and OH^-, respectively [69, 70]. The presence of these Fe and O peaks indicates that the possible existence of FeO, Fe_2O_3, Fe_3O_4 and FeOOH in the corrosion products. However, it is difficult to differentiate some of these iron compounds, such as γ-Fe_2O_3, γ-FeOOH and α-FeOOH, by XPS [71]. Further identification of the exact compounds formed in the corrosion products was, thus, performed by Raman spectroscopy which are presented in the next section. Furthermore, the P 2p peak at 133.2 eV in XPS spectra can be assigned to PO_4^{3-} in the corrosion products [72].

To compare the composition of the corrosion products formed at different M/P ratios, the Fe^{2+}/Fe^{3+}, O^{2-}/OH^- and P/Fe ratios calculated from the XPS spectra in Fig. 8 are presented in Fig. 9. As can be observed, the P/Fe ratio of M/P 17 specimen is significantly lower than those of M/Ps 7 and 12 specimens. This indicates that a higher M/P ratio, such as M/P 17, can result in a much-reduced content of iron phosphate in the corrosion products, which could be attributed to the significantly reduced phosphate content in M/P 17 pore solution compared to those of M/Ps 7 and 12 (as shown in Table 4). This is in agreement with the literature which reported that the HPO_4^{2-}/PO_4^{3-} ions at a low concentration (e.g., 10 mmol/l) can inhibit the corrosion of steel by physical or/and chemical adsorption onto steel surface [27], while at high concentration, HPO_4^{2-}/PO_4^{3-} ions (e.g., 20-100 mmol/l) can precipitate as a corrosion product to inhibit any further corrosion [26]. Furthermore, as shown in Fig. 9, in general both the Fe^{2+}/Fe^{3+} and O^{2-}/OH^- ratios also decrease with an increase of M/P ratio, which indicates that a lower M/P ratio can possibly facilitate the formation of ferric hydroxide in the corrosion products. This could be related to the increased HPO_4^{2-}/PO_4^{3-} content at a lower M/P ratio, which can promote its reaction with the iron ions dissolved from the steel substrate to form iron phosphate compounds. However, as the Gibbs free energy of $Fe_3(PO_4)_2$ (–2444.80 kJ/mol)

is much lower than that of $FePO_4$ (-1657.70 kJ/mol) and $FeHPO_4$ [73-75], the formation of $Fe_3(PO_4)_2$, thus, would dominate the corrosion reaction. On the other hand, it was reported that the presence of HPO_4^{2-}/PO_4^{3-} ions could inhibit the formation of FeOOH, whilst the formation of iron oxides could be promoted [58]. The above can explain the reason that the corrosion products formed at a lower M/P ratio exhibit higher Fe^{2+}/Fe^{3+} and O^{2-}/OH^- ratios. As a comparison, the Fe^{2+}/Fe^{3+} and O^{2-}/OH^- ratios of the corrosion products formed in the PC pore solution are higher than those in M/P 17 pore solution. This suggests that the corrosion products formed in PC pore solution possibly have a lower content of ferric hydroxide than that formed in M/P 17 pore solution. It should be noted that the corrosion products only appeared at localized areas on the surface of mild steel in the MKPC pore solutions, while most part of the mild steel in PC pore solution was severely corroded. This distinct difference in the corrosion performance of mild steel in MKPC and PC could be related to the presence of HPO_4^{2-}/PO_4^{3-} ions in the MKPC pore solutions as discussed in detail in Section 3.7.

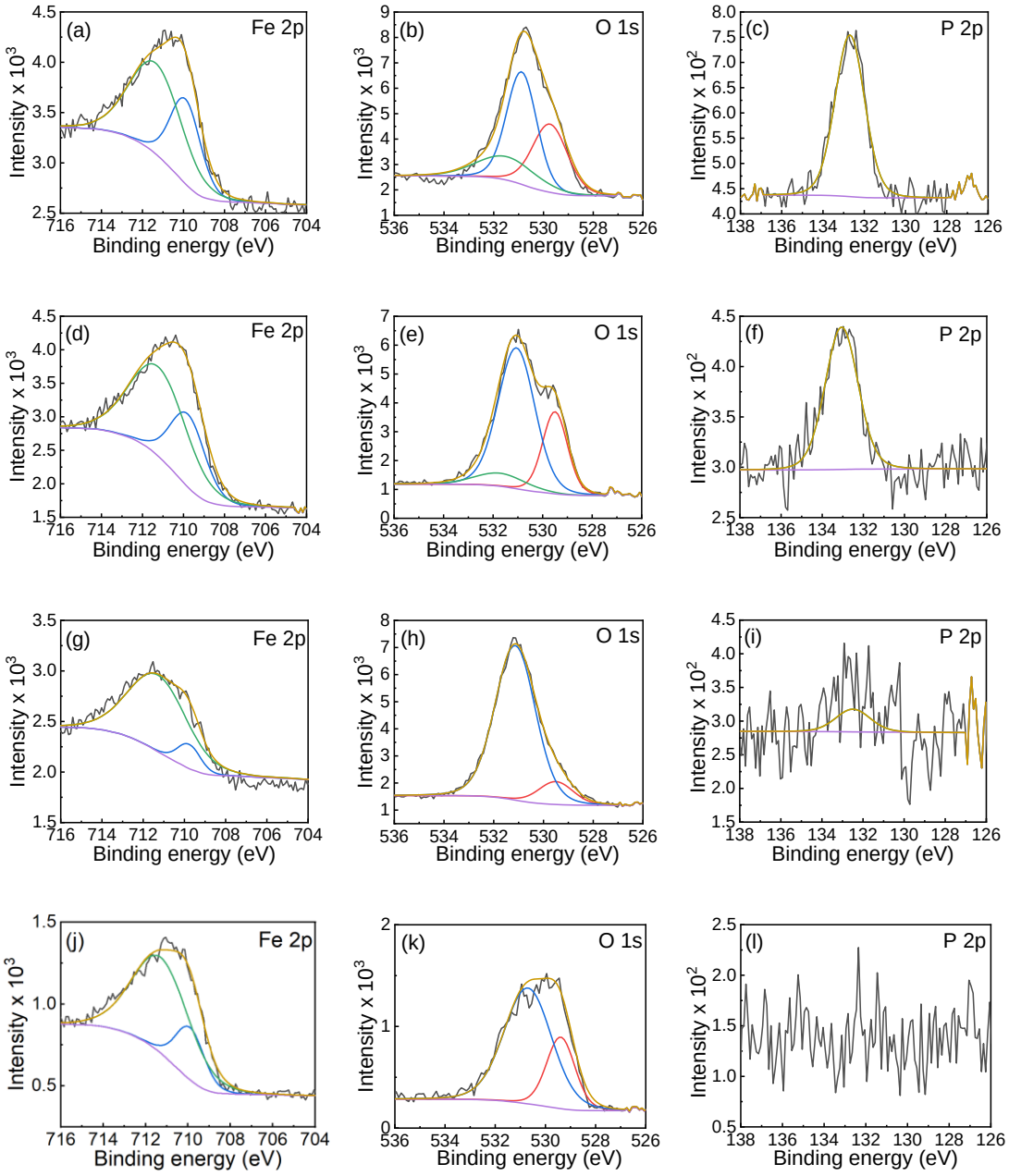

Fig. 8. XPS spectra of the corrosion products formed on the mild steel in the MKPC and PC pore solutions containing chloride ions: (a)-(c) M/P 7; (d)-(f) M/P 12; (g)-(i) M/P 17; and (j)-(l) PC

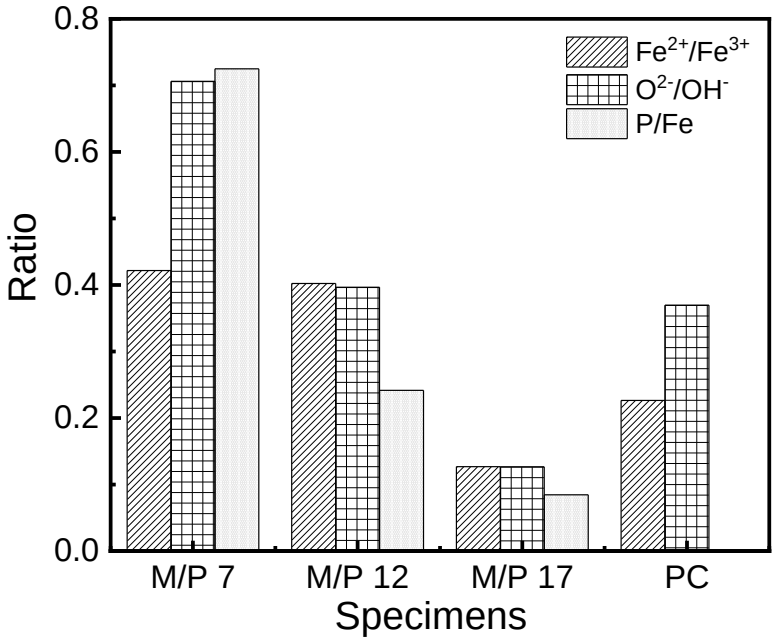

Fig. 9. Comparison of the composition of the corrosion products formed on the mild steel in the MKPC and PC pore solutions containing 1.4 M chloride ions

However, it must be emphasized that, although thermodynamically the formation of $Fe_3(PO_4)_2$ as the dominant product is preferred during both the passivation and corrosion of steel in MKPC systems with low M/P [39, 76-78], there are differences in the exact composition between the products formed in the passive film and corrosion products. Fig. 10 compares the composition of the corrosion products identified in the current study with those of the passive films formed in MKPC reported by the authors in a previous study [16]. It can be seen that the P/Fe ratios of the corrosion products are all higher than those of the passive films, indicating that the relative amounts of iron phosphates formed in the corrosion products are higher than those in the passive films. The increased P/Fe in the corrosion products as identified in the current study could be mainly attributed to the reduced stability of iron oxide/hydroxides in the presence of Cl^-. As indicated below, based on Gibb's free energy, not only the stability $Fe_3(PO_4)_2$ is much higher than that of iron oxide/hydroxides, but Cl^- ions could also promote the conversion of iron oxide/hydroxides [79] to $Fe_3(PO_4)_2$, leading to a higher P/Fe than that of the passive film (as to be further discussed below). On the other hand, the Fe^{2+}/Fe^{3+} ratios

of corrosion products are all lower than those of passive films. This pattern is similar to those reported in the corrosion of steel in PC systems [80] which could be primarily attributed to the increased availability of O_2 during the solid-state growth stage of the corrosion process [81]. As a result, the oxidation rate of Fe^{2+} ions in the corrosion products is much higher than that in the passive film, which leads to an increased ferric compounds in the corrosion products. The above comparison in the composition of the products formed during the passivation and corrosion of steel in MKPC systems would suggest, different from those well-established theories in PC system, due to the unique pore solution chemistry of MKPC, different mechanisms have occurred during the de-passivation and corrosion of steel in MKPC systems which will be discussed in detail in the following sections.

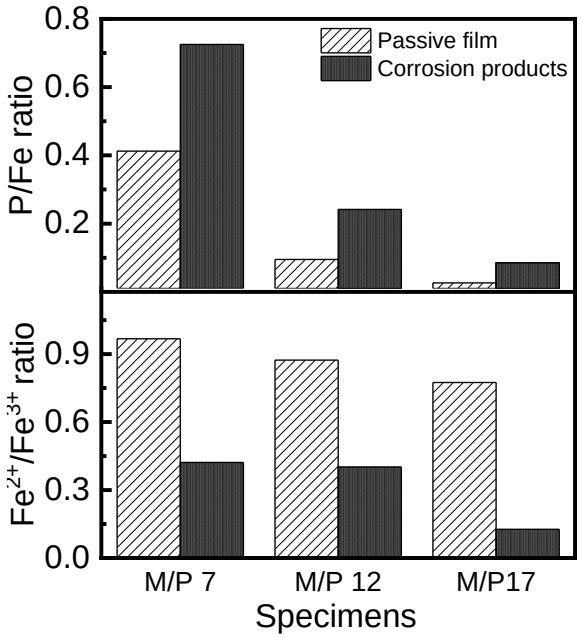

Fig. 10. Comparison between the compositions of passive films obtained from [16] and that of corrosion products obtained from this study

3.6.2 Raman spectroscopy

The possible corrosion products formed on the mild steel in the MKPC and PC pore solutions containing 1.4 M chloride ions were further identified via Raman spectroscopy because

Raman spectroscopy can provide fingerprint information on the molecular structures of materials and thus can identify the corrosion products. The obtained Raman spectra are shown in Fig. 11. As can be observed from Figs. 11(a)-(c), the Raman spectra of M/Ps 7, 12 and 17 specimens exhibit the peaks at around 309 cm^{-1}, 389 cm^{-1}, 534 cm^{-1} and 725 cm^{-1}, which can be assigned to the characteristic peaks of akageneite (β-FeOOH) [82-84]. The presence of the peaks at around 489 cm^{-1} for M/Ps 7, 12 and 17 specimens can be assigned to the Fe–OH asymmetrical stretching vibration of goethite (α-FeOOH) [85]. Moreover, the peak at around 661 cm^{-1} appears in the Raman spectra of M/Ps 7 and 12 specimens, which can be assigned to the Fe-O symmetrical stretching in T sites of magnetite (Fe_3O_4) [86]. Additionally, the peaks at around 411 cm^{-1} and 607 cm^{-1} can be attributed to the two Fe-O symmetrical bending vibrations of hematite (α-Fe_2O_3) [87]. However, the presence of α-Fe_2O_3 is generally believed to be attributed to the heating of lasers when the Raman spectroscopy is performed [88]. Overall, it can be concluded from the Raman spectra that β-FeOOH and α-FeOOH mainly exists in the corrosion products for all the MKPC specimens. In addition to this, Fe_3O_4 also formed in the M/Ps 7 and 12 specimens. The above results are consistent with the literature which showed that Fe_3O_4 and FeOOH presented in the corrosion products formed in the alkaline solutions containing HPO_4^{2-}/PO_4^{3-} ions [26, 58].

Compared with the Raman spectrum of M/P 17 specimen, the spectra of M/Ps 7 and 12 specimens exhibit an additional peak at 911 cm^{-1}, which corresponds to symmetric stretching mode of PO_4 [89]. This would indicate that iron phosphate compounds were formed in the corrosion products of M/Ps 7 and 12 specimens, which correlates well with the XPS results in Fig. 8.

Fig. 11(d) shows the Raman spectrum of the mild steel immersed in the PC pore solution containing 1.4 M chloride ions. As can be seen, the pattern of the Raman spectrum of PC

specimen is obviously different from those of the M/Ps 7, 12 and 17 specimens. The Raman peaks at 230 cm^{-1}, 299 cm^{-1} and 698 cm^{-1} can be noticed in Fig. 11(d), which can be assigned to the Fe-O symmetrical stretching, Fe-OH symmetrical bending and Fe–O symmetrical stretching vibrations of goethite (α-FeOOH), respectively [87]. Moreover, the peaks at 389 cm^{-1} and 658 cm^{-1} can be assigned to lepidocrocite (γ-FeOOH), similar to those reported in the literature [90]. This implies that the chloride-induced corrosion of mild steel in PC mainly leads to the formation of several types of FeOOH, including α-FeOOH and γ-FeOOH, in the corrosion products [91, 92].

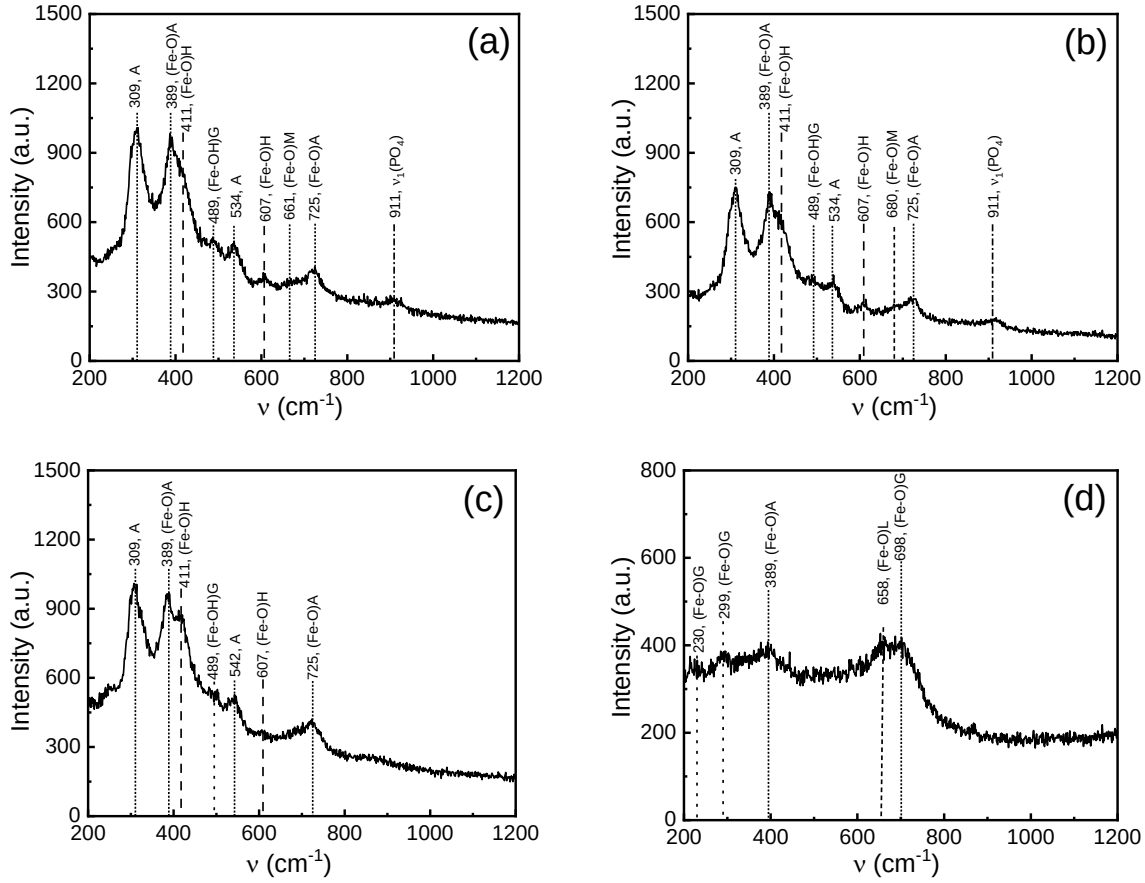

Fig. 11. Raman spectra of the corrosion products formed on the mild steel in the MKPC and PC pore solutions containing 1.4 M chloride ions: (a) M/P 7; (b) M/P 12; (c) M/P 17; and (d) PC (Note: A—Akageneite, H—Hematite, G—Goethite, M--Magnetite)

3.7 The corrosion mechanism of the mild steel in the MKPC pore solutions

As mentioned before, it is generally believed that the resistance of mild steel to chloride-induced corrosion increases with increasing pH and a pH value of above 10.5~11.5 is considered essential for the formation of a stable oxide film to resist the chloride-induced corrosion [93]. In this study, the measured pH of the MKPC pore solutions ranged from 8.69 to 10.29, which is obviously lower, and even much lower, than that of the PC specimen (pH =12.89). This is also lower than what is expected for the passivation of steel. Therefore, the mild steel in MKPC is anticipated to show poor resistance to chloride-induced corrosion. However, the electrochemical results in Sections 3.2 and 3.3 showed that the corrosion resistance of mild steel in MKPC is actually higher than that in PC. To further confirm this unexpected observation, the critical chloride values of mild steel reported in PC systems were collected from the literature and compared in Fig. 12 with those obtained from the MKPC and PC systems in the current study. As can be observed from Fig. 12, although the pH values of the MKPC are much lower than those of PC, the critical chloride values of the mild steel in MKPC are actually higher than those in PC, indicating that the resistance of mild steel to chloride-induced depassivation and corrosion in MKPC is higher than that in PC. This is, obviously, contradictory to what has been claimed in the literature which confirmed that the decreased pH reduces the protective capability of the passive film of steel [94]. However, based on the results presented in this paper, it is the authors' view that this contradiction could be attributed to the phosphates existing in MKPC systems (as further elaborated below). Nonetheless, the fitting curves for both PC and MKPC specimens in Fig. 12 still show a linear relationship between the critical chloride value and pH (although different trends have been identified for PC and MKPC), which is consistent with the pattern reported for steel corrosion in PC [22]. This demonstrates that the increased pH of MKPC can also increase the resistance of mild steel to chloride-induced corrosion. However, the slope of the fitting curve for the MKPC specimens is much higher than that for PC specimens, indicating that pH may have a less significant effect on chloride-induced corrosion in MKPC system compared to that in PC and

something else may have also played a role. To clearly understand the possible mechanisms involved in the chloride-induced corrosion of mild steel in MKPC systems, the depassivation and corrosion mechanisms of mild steel in MKPC are further discussed in detail below.

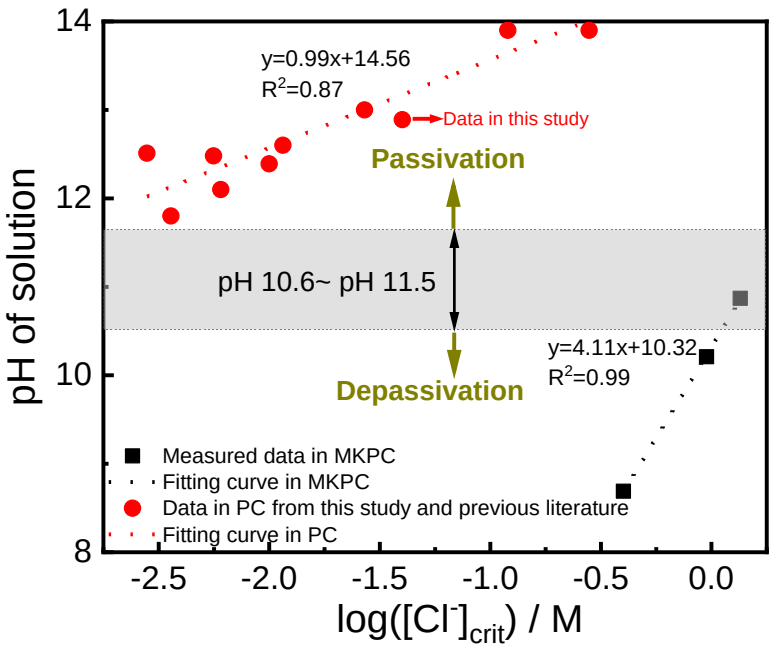

Fig. 12. Comparison between the critical chloride values in MKPC and those in PC, as a function of pH (The data for PC were obtained from this study and the previous literature [22, 51, 95, 96])

One of the main differences in the composition of pore solution between PC and MKPC is that HPO_4^{2-}/PO_4^{3-} ions exist in all the MKPC pore solutions (as demonstrated in Table 4).

In order to clearly illustrate the possible effects of M/P ratio on the depassivation and corrosion mechanisms of the mild steel in MKPC pore solutions, the passivation, depassivation and corrosion process of the mild steel in low and high M/P ratios as well as in PC pore solution are separately proposed and schematically shown in Fig. 13. As shown in Figs. 13(a) and (d), it has been established in a previous study that the passive film formed in low M/P (i.e., M/Ps 7 and 12) mainly consists of iron phosphates and iron oxides/hydroxides, while that in high M/P ratio (i.e., M/P 17) consists of iron oxides/hydroxides (i.e., γ-Fe2O3 and α-FeOOH) [16].

As a comparison, the passive film formed in PC is commonly considered to be composed of iron oxides/hydroxides [94] as illustrated in Fig. 13(g). Since a higher pH has been reported to favour the formation of more compact passive film in PC system [94], it can be deduced that the iron oxides/hydroxides in the passive film formed in PC should be more compact than those formed in MKPC due to the lower pH environment of the MKPC system. Therefore, it is anticipated that the protective capability of the passive film formed in PC must be higher than those formed in MKPC. However, as shown in the electrochemical results in Fig. 4(a-1) and (a-2), the protective capability of the passive film formed in MKPC is actually higher than that formed in PC. This could be related to the presence of HPO_4^{2-}/PO_4^{3-} ions in the MKPC pore solutions, which can compete with the OH^- ions and preferentially adsorb on the surface of passive film [16], resulting in an increased protective capacity of passive film [97]. It should be noted that even at a very low concentration, such as 10^{-3} M, HPO_4^{2-}/PO_4^{3-} ions still can adsorb on the surface of the iron hydroxide in an alkaline solution [98]. This implies that, even though the concentration of HPO_4^{2-}/PO_4^{3-} ions in M/P 17 pore solution is much lower (5×10^{-3} M) than those in M/Ps 12 (0.209 M) and 7 (1.127 M), the HPO_4^{2-}/PO_4^{3-} ions could still be able to adsorb on the surface of passive film formed in M/P 17 pore solution. Similar observation has also been reported in a previous study which showed that the HPO_4^{2-}/PO_4^{3-} ions can easily adsorb on the surface of iron oxides/hydroxides [99]. Therefore, it is mainly due to the adsorbed HPO_4^{2-}/PO_4^{3-} ions which has resulted in a higher passivity of the mild steel in all the MKPC systems investigated in this study than that in PC as demonstrated in Figs. 4(a-1) and (a-2). However, even though HPO_4^{2-}/PO_4^{3-} ions can adsorb on the passive films formed in both low and high M/P ratios, it must be emphasized that the microstructure of the iron oxides/hydroxides in passive film is primarily affected by pH [94]. Therefore, the iron oxides/hydroxides in the passive film formed in low M/P ratio could be more porous than those in high M/P ratio due to the lower pH of the pore solution with low M/P ratio. This could explain the relatively lower passivity of the mild steel in low M/P ratio compared to that in high M/P ratio as shown in Figs. 4(a-1) and (a-2). However, detailed microstructural analysis of the

passive films formed under different M/P ratios still needs to be systematically studied in the future.

In the presence of Cl^-, it is well known that Cl^- ions could compete with HPO_4^{2-}/PO_4^{3-} and OH^- ions to occupy the sites on the surface of steel passive film, which could lead to a complex depassivation mechanism of steel reinforcement [26]. Based on the Gibbs free energy ΔG for the formation of various iron compounds (as shown in Eqs.3-5) [39, 76-78], it could be deduced that the stability of the compounds which could possibly be formed in the presence of anions such as Cl^-, PO_4^{3-} and OH^- ions can be ranked (in the order from high to low) as: $Fe_3(PO_4)_2$>>$FeCl_2$>$Fe(OH)_2$. Since the ΔG of $Fe_3(PO_4)_2$ is much higher than that of $FeCl_2$, this indicates that, at a lower M/P ratio (e.g., 7 and 12), it is difficult for Cl^- ions to react with the iron phosphate component in the passive film to form $FeCl_2$, which can inhibit the dissolution of $Fe_3(PO_4)_2$ and subsequent breakdown of passive film at these sites. On the other hand, the adsorption of PO_4^{3-} ions on the surface of iron oxides/hydroxides component on the passive film formed at M/P ratios of 7 and 12 also makes these sites less available for the adsorption of Cl^- ions (as schematically shown in Figs. 13(b) and (e)). As a result, the adsorption of Cl^- ions can only occur at some sites where the adsorption of PO_4^{3-} ions is inadequate [100]. Similar mechanisms could also occur with M/P ratio of 17, however, in that case, the $Fe_3(PO_4)_2$ is not formed. It should be noted that since the iron oxides/hydroxides in the passive film formed in high M/P ratio are possibly more compact than those formed in low M/P ratio [16], this could lead to a higher resistance to the penetration by Cl^- ions than those in low M/P ratios, as schematically illustrated in Figs. 13(b) and (e). Based on the penetration mechanism of depassivation [101], the reduced penetration of Cl^- ions through the passive film formed in M/P 17 would imply that the formation of soluble $FeCl_2$ complexes and subsequent precipitation of expansive corrosion products at these sites should be reduced. This hypothesis, as schematically presented in Figs. 13(c) and (f), can be clearly verified by the localized corrosion shown in the SEM images in Fig. 7. On the other hand, as highlighted before, the presence of

HPO_4^{2-}/PO_4^{3-} ions in the MKPC pore solutions is also believed to be able to reduce the activity coefficient of chloride ions and, thus, decrease the effective chloride concentration, which could also contribute to the increased resistance of the steel to chloride attack [49].

$$3Fe^{2+} + 2PO_4^{3-} \rightarrow Fe_3(PO_4)_2 \qquad \Delta G = -2444.80 \text{ kJ/mol} \qquad \text{Eq. 3}$$

$$2Fe^{2+} + Cl^{-} \rightarrow FeCl_2 \qquad \Delta G = -302.35 \text{ kJ/mol} \qquad \text{Eq. 4}$$

$$Fe^{2+} + OH^{-} \rightarrow Fe(OH)_2 \qquad \Delta G = -195.00 \text{ kJ/mol} \qquad \text{Eq. 5}$$

Due to the different depassivation mechanisms as discussed above, there are also some distinct differences in the subsequent chloride-induced corrosion of the mild steel in the MKPC systems with different M/P ratios. As the Δ*G* of $Fe_3(PO_4)_2$ is much more negative than that of $Fe(OH)_2$ (as shown Eq. 5), the presence of considerable amounts of HPO_4^{2-}/PO_4^{3-} ions in the pore solution of low M/P ratios (i.e., 7 and 12) would indicate that the reaction between the dissolved iron and HPO_4^{2-}/PO_4^{3-} ions is more preferred. Moreover, according to the equilibrium diagram of the iron(II)-phosphate system [75], the dominant precipitate in the pH range of 8.69 to 10.87 has found indeed to be $Fe_3(PO_4)_2$ compounds which had also been confirmed by other researchers in their studies [41, 102].

This explains the finding in this study that $Fe_3(PO_4)_2$ has been identified as the dominant corrosion products in the MKPC systems with M/Ps of 7 and 12. In contrast, the low concentration of HPO_4^{2-}/PO_4^{3-} ions in the pore solution of M/P 17 leads to the formation of little $Fe_3(PO_4)_2$. Instead, the formation of iron oxide and hydroxide has dominated its corrosion mechanism as demonstrated by the results of XPS and Raman spectroscopy. Nonetheless, due to the inhibiting role played by HPO_4^{2-}/PO_4^{3-} ions, only localised corrosion can be formed in the MKPC systems, regardless of its M/P ratio [26], as evidenced by the SEM images in Fig.

7(c). In comparison, as shown in Fig. 7(d), more severe corrosion can be observed on the whole surface of mild steel in chloride-laden PC pore solution. This distinctly different feature could be mainly attributed to the absence of HPO_4^{2-}/PO_4^{3-} ions in PC system. As a result, Cl^- ions can be easily adsorbed on the surface of passive film. According to the adsorption mechanism of depassivation [103], due to the formation of soluble $FeCl_2$ complexes, the breakdown of passive film occurs. These soluble $FeCl_2$ complexes could then react with the OH^- ions in the PC pore solutions to form insoluble iron hydroxides as the main corrosion products [80, 104], as schematically illustrated in Fig. 13(i) and also evidenced by the results of XPS (Fig. 8) and Raman spectroscopy (Fig. 11).

Overall, based on the results presented in this study, it can be concluded that, despite of much lower pH values, MKPC system contributes to a significantly enhanced corrosion resistance of mild steel compared with that in PC system, which could be mainly attributed to the inhibiting roles played by the HPO_4^{2-}/PO_4^{3-} ions in the pore solution of MKPC systems. Whilst both pH and HPO_4^{2-}/PO_4^{3-} content are key factors influencing the chloride-induced depassivation and corrosion of mild steel in the MKPC systems, pH still plays the dominant role with a higher pH favouring an increased resistance to corrosion. Therefore, in terms of the resistance to chloride-induced corrosion, higher M/P is preferred when designing MKPC for durability-related applications. Nonetheless, it must be noted that the compressive strength of MKPC is not a simple monotonic function of M/P. At a given water/solid, there is always an optimal M/P existing for the highest compressive strength [20]. In other words, when an optimal M/P is required to increase the resistance to chloride-induced corrosion of the mild steel in MKPC, a balance is also needed in order to ensure that the compressive strength will not suffer. However, it must be emphasized that based on the data obtained in this study, MKPC has demonstrated a better protection to the steel reinforcement than that in PC, showing a great potential for its application under marine environment.

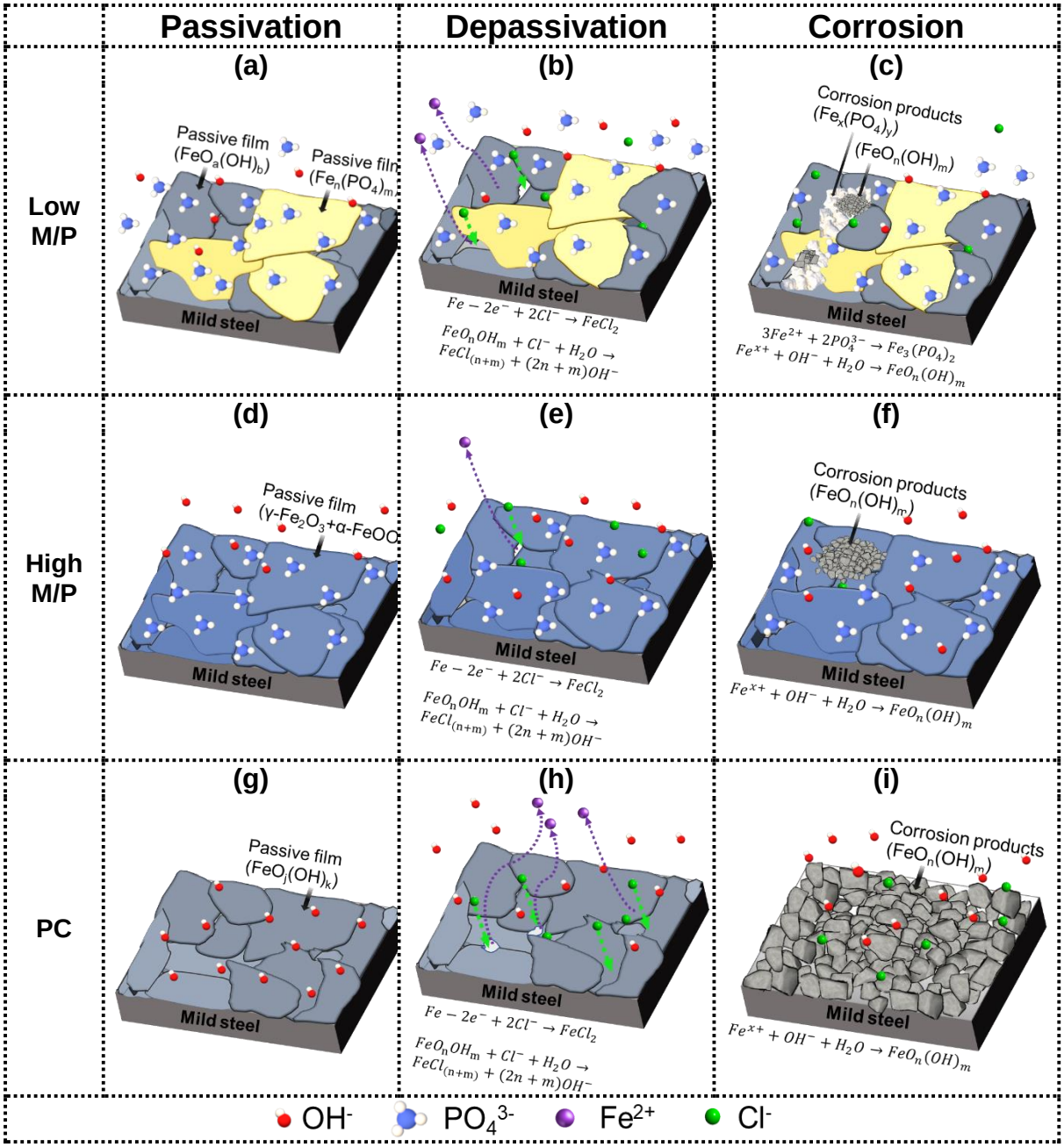

Fig. 13. Proposed chloride-induced depassivation and corrosion mechanisms of mild steel in MKPC as compared with that in PC systems: (a) the passive film formed in low M/P MKPC, showing iron hydroxide/oxide and iron phosphate compounds as the main products; (b) depassivation of passive film in low M/P MKPC, showing the complexation and penetration by chloride at the localized sites consisting of iron hydroxide/oxide; (c) localised corrosion of steel in low M/P MKPC, showing iron hydroxide/oxide and iron phosphate compounds formed as the main corrosion products; (d) the passive film formed in high M/P MKPC, showing iron hydroxide/oxide as the main products; (e) depassivation of passive film in high M/P MKPC, showing the release of iron ions at localised sites under the competitive adsorption of chloride, hydroxyl and phosphate ions; (f) localized corrosion of steel in high M/P MKPC, showing iron hydroxide/oxide formed as the main corrosion products; (g) the passive film formed in PC, showing iron oxide/hydroxide as the main products; (h) depassivation of passive film in PC,

showing the intensive release of iron ions in the absence of HPO_4^{2-}/PO_4^{3-} ions; and (i) general corrosion of steel in PC, showing massive formation of iron hydroxide/oxide as the main corrosion products . (Note: only the ions playing the dominant roles in the passivation, depassivation and corrosion of steel are shown in Fig. 13)

4 Conclusions

In this paper, the chloride-induced depassivation and corrosion behaviour of mild steel in MKPC cements with different M/P ratios was investigated with several electrochemical methods, including OCP, LPR, EIS and potentiodynamic polarisation. The corrosion products formed were also characterised by Raman spectroscopy, SEM/EDS and XPS. Based on the results obtained, the following conclusions can be drawn:

a) Although the pH of MKPC is much lower than that of PC, the resistance of mild steel to chloride-induced attack is significantly higher in MKPC pore solutions than that in PC pore solution. In particular, the critical chloride values in MKPC have found to be several orders higher than that in PC. The superior protection provided by MKPC to mild steel is mainly attributed to the inhibiting role played by the HPO_4^{2-}/PO_4^{3-} ions.
b) The corrosion products formed in the MKPC with M/P ratios 7 and 12 are mainly composed of iron phosphate and iron hydroxide/oxide, while those in the MKPC with M/P ratio of 17 mainly consist of iron hydroxide/oxide. The formation of different corrosion products is mainly dominated by the HPO_4^{2-}/PO_4^{3-} concentration in the pore solution, which is, in turn, determined by the M/P ratios of MKPC.
c) Whilst M/P ratio of MKPC plays an important role in determining the depassivation and corrosion behaviour as well as the corrosion products of steel under the attack of chloride ions, the pH of the pore solution is still the most important factor in determining the protective capacity of steel. Therefore, a higher M/P can benefit the resistance to chloride-induced depassivation and corrosion. However, as the compressive strength of MKPC is

not a simple monotonic function of M/P, a suitable M/P to balance the durability and mechanical properties of MKPC is needed for practical applications.

d) Based on the data obtained in this study, MKPC has demonstrated a great potential for its application under marine environment where a good resistance to chloride-induced corrision is paramountly important.

5 Acknowledgement

The authors are most thankful to the financial supports received for this research from UK Engineering and Physical Sciences Research Council (EPSRC) (Grant No. EP/M003159/1) and National Natural Science Foundation of China (NSFC) (51461135003) under the EPSRC-NSFC Collaborative Research Scheme on ‘Sustainable Materials for Infrastructure’. The China Scholarship Council and UCL Faculty of Engineering Sciences are gratefully acknowledged for providing the studentship for Miss Danqian Wang’s PhD study at UCL. Mr Warren Gaynor, Dr Shi Shi and Dr Judith Zhou at UCL are also gratefully acknowledged for their help with the experiment work.

Data availability

The raw/processed data required to reproduce these findings cannot be shared at this time as the data also forms part of an ongoing study.

Reference

[1] A. Poursaee, C.M. Hansson, Reinforcing steel passivation in mortar and pore solution, Cem. Concr. Res., 37 (2007) 1127-1133.

[2] S. Joiret, M. Keddam, X.R. Nóvoa, M.C. Pérez, C. Rangel, H. Takenouti, Use of EIS, ring-disk electrode, EQCM and Raman spectroscopy to study the film of oxides formed on iron in 1 M NaOH, Cem. Concr. Compos., 24 (2002) 7-15.

[3] Z. Ai, W. Sun, J. Jiang, D. Song, H. Ma, J. Zhang, D. Wang, Passivation characteristics of alloy corrosion-resistant steel Cr10Mo1 in simulating concrete pore solutions: combination effects of pH and chloride, Materials, 9 (2016) 749.

[4] J. Xu, L. Jiang, W. Wang, Y. Jiang, Influence of $CaCl_2$ and NaCl from different sources on chloride threshold value for the corrosion of steel reinforcement in concrete, Constr Build Mater., 25 (2011) 663-669.

[5] A. Köliö, M. Honkanen, J. Lahdensivu, M. Vippola, M. Pentti, Corrosion products of carbonation induced corrosion in existing reinforced concrete facades, Cem. Concr. Res., 78 (2015) 200-207.

[6] I. Fernandez, M. Etxeberria, A.R. Marí, Ultimate bond strength assessment of uncorroded and corroded reinforced recycled aggregate concretes, Constr Build Mater., 111 (2016) 543-555.

[7] S. Mundra, M. Criado, S.A. Bernal, J.L. Provis, Chloride-induced corrosion of steel rebars in simulated pore solutions of alkali-activated concretes, Cem. Concr. Res., 100 (2017) 385-397.

[8] C. Fang, K. Gylltoft, K. Lundgren, M. Plos, Effect of corrosion on bond in reinforced concrete under cyclic loading, Cem. Concr. Res., 36 (2006) 548-555.

[9] B.S. EN, Concrete–Specification, performance, production and conformity, (2013).

[10] B.S. Institution, Concrete--complementary British Standard to BS EN 206-1: Method of Specifying and Guidance for the Specifier, BSI2006.

[11] S.S. Seehra, S. Gupta, S. Kumar, Rapid setting magnesium phosphate cement for quick repair of concrete pavements — characterisation and durability aspects, Cem. Concr. Res., 23 (1993) 254-266.

[12] J. Qin, J. Qian, C. You, Y. Fan, Z. Li, H. Wang, Bond behavior and interfacial micro-characteristics of magnesium phosphate cement onto old concrete substrate, Constr Build Mater., 167 (2018) 166-176.

[13] C. Yu, Q. Wu, J. Yang, Effect of seawater for mixing on properties of potassium magnesium phosphate cement paste, Constr Build Mater., 155 (2017) 217-227.

[14] W. Sun, Y. Zheng, L. Zhou, J. Song, Y. Bai, A study of the bond behavior of FRP bars in MPC seawater concrete, Adv. Struct. Eng, 24 (2021) 1110-1123.

[15] C. McCague, Development of novel composite cement systems for the encapsulation of aluminium from nuclear wastes, Queen's University Belfast, 2015.

[16] D. Wang, Y. Yue, T. Mi, S. Yang, C. McCague, J. Qian, Y. Bai, Effect of magnesia-to-phosphate ratio on the passivation of mild steel in magnesium potassium phosphate cement, Corros. Sci., 174 (2020) 108848.

[17] H. Pei, Z. Li, J. Zhang, Q. Wang, Performance investigations of reinforced magnesium phosphate concrete beams under accelerated corrosion conditions by multi techniques, Constr Build Mater., 93 (2015) 989-994.

[18] J. Zhang, H. Ma, H. Pei, Z. Li, Steel corrosion in magnesia–phosphate cement concrete beams, Magazine of Concrete Research, 69 (2017) 35-45.

[19] M. Le Rouzic, T. Chaussadent, L. Stefan, M. Saillio, On the influence of Mg/P ratio on the properties and durability of magnesium potassium phosphate cement pastes, Cem. Concr. Res., 96 (2017) 27-41.

[20] H. Ma, B. Xu, J. Liu, H. Pei, Z. Li, Effects of water content, magnesia-to-phosphate molar ratio and age on pore structure, strength and permeability of magnesium potassium phosphate cement paste, Mater. Des., 64 (2014) 497-502.

[21] L. Chong, C. Shi, J. Yang, H. Jia, Effect of limestone powder on the water stability of magnesium phosphate cement-based materials, Constr Build Mater., 148 (2017) 590-598.

[22] V.K. Gouda, Corrosion and Corrosion Inhibition of Reinforcing Steel: I. Immersed in Alkaline Solutions, Br. Corros. J., 5 (1970) 198-203.

[23] J. Shi, W. Sun, Effects of phosphate on the chloride-induced corrosion behavior of reinforcing steel in mortars, Cem. Concr. Compos., 45 (2014) 166-175.

[24] S.A.M. Refaey, S.S. Abd El-Rehim, F. Taha, M.B. Saleh, R.A. Ahmed, Inhibition of chloride localized corrosion of mild steel by PO_4^{3-}, CrO_4^{2-}, MoO_4^{2-}, and NO^{2-} anions, Applied Surface Science, 158 (2000) 190-196.

[25] S.A.M. Refaey, Inhibition of steel pitting corrosion in HCl by some inorganic anions, Applied Surface Science, 240 (2005) 396-404.

[26] L. Yohai, W. Schreiner, M. Vázquez, M.B. Valcarce, Phosphate ions as effective inhibitors for carbon steel in carbonated solutions contaminated with chloride ions, Electrochimica Acta, 202 (2016) 231-242.

[27] A. Mohagheghi, R. Arefinia, Corrosion inhibition of carbon steel by dipotassium hydrogen phosphate in alkaline solutions with low chloride contamination, Constr Build Mater., 187 (2018) 760-772.

[28] L. Yohai, M. Vázquez, M.B. Valcarce, Phosphate ions as corrosion inhibitors for reinforcement steel in chloride-rich environments, Electrochimica Acta, 102 (2013) 88-96.

[29] H. Tang, J. Qian, Z. Ji, X. Dai, Z. Li, The protective effect of magnesium phosphate cement on steel corrosion, Constr Build Mater., 255 (2020) 119422.

[30] S. Yin, H. Yang, Y. Dong, C. Qu, J. Liu, T. Guo, K. Duan, Environmentally favorable magnesium phosphate anti-corrosive coating on carbon steel and protective mechanisms, Sci. Rep., 11 (2021) 197.

[31] G. Zhang, G. Li, T. He, Effects of sulphoaluminate cement on the strength and water stability of magnesium potassium phosphate cement, Constr Build Mater., 132 (2017) 335-342.

[32] P. Longuet, La Phase Liquide du Ciment Hydrate Rev.des Materiaux de Constructions et des Travaux Publics, Ciments et Betons, 676 (1973) 35-41.

[33] P. Longuet, La phase liquide du ciment hydraté, (1973).

[34] R.S. Barneyback, S. Diamond, Expression and analysis of pore fluids from hardened cement pastes and mortars, Cem. Concr. Res., 11 (1981) 279-285.

[35] A. Vollpracht, B. Lothenbach, R. Snellings, J. Haufe, The pore solution of blended cements: a review, Mater. Struct., 49 (2016) 3341-3367.

[36] H. Yu, K.-T.K. Chiang, L. Yang, Threshold chloride level and characteristics of reinforcement corrosion initiation in simulated concrete pore solutions, Constr Build Mater., 26 (2012) 723-729.

[37] N. Boucherit, A. Hugot-Le Goff, S. Joiret, Raman studies of corrosion films grown on Fe and Fe-6Mo in pitting conditions, Corros. Sci., 32 (1991) 497-507.

[38] Y. Zuo, H. Wang, J. Zhao, J. Xiong, The effects of some anions on metastable pitting of 316L stainless steel, Corros. Sci., 44 (2002) 13-24.

[39] V.B. Parker, I.L. Khodakovskii, Thermodynamic properties of the aqueous ions (2+ and 3+) of iron and the key compounds of iron, Journal of Physical and Chemical Reference Data, 24 (1995) 1699-1745.

[40] P. Hajos, O. Horvath, V. Denke, Prediction of retention for halide anions and oxoanions in suppressed ion chromatography using multiple species eluent, Analytical Chemistry, 67 (1995) 434-441.

[41] C.A. Melendres, N. Camillone, T. Tipton, Laser raman spectroelectrochemical studies of anodic corrosion and film formation on iron in phosphate solutions, Electrochimica Acta, 34 (1989) 281-286.

[42] M.K. Seliem, S. Komarneni, M.R.A. Khadra, Phosphate removal from solution by composite of MCM-41 silica with rice husk: kinetic and equilibrium studies, Microporous Mesoporous Mater., 224 (2016) 51-57.

[43] B. Xu, B. Lothenbach, A. Leemann, F. Winnefeld, Reaction mechanism of magnesium potassium phosphate cement with high magnesium-to-phosphate ratio, Cem. Concr. Res., 108 (2018) 140-151.

[44] H. Lahalle, C. Patapy, M. Glid, G. Renaudin, M. Cyr, Microstructural evolution/durability of magnesium phosphate cement paste over time in neutral and basic environments, Cem. Concr. Res., 122 (2019) 42-58.

[45] M. Sánchez, J. Gregori, C. Alonso, J.J. García-Jareño, H. Takenouti, F. Vicente, Electrochemical impedance spectroscopy for studying passive layers on steel rebars immersed in alkaline solutions simulating concrete pores, Electrochimica Acta, 52 (2007) 7634-7641.

[46] J. Williamson, O.B. Isgor, The effect of simulated concrete pore solution composition and chlorides on the electronic properties of passive films on carbon steel rebar, Corros. Sci., 106 (2016) 82-95.

[47] L. Li, A.A. Sagüés, Chloride corrosion threshold of reinforcing steel in alkaline solutions—open-circuit immersion tests, Corrosion, 57 (2001) 19-28.

[48] C. Andrade, C. Alonso, Test methods for on-site corrosion rate measurement of steel reinforcement in concrete by means of the polarization resistance method, Mater. Struct., 37 (2004) 623-643.

[49] R. Wang, F. He, C. Chen, L. Dai, Coupling effect of the connected pores and pore solution on chloride ion migration in cement-based materials, Constr Build Mater., 297 (2021) 123773.

[50] J. Xu, L. Jiang, J. Wang, Influence of detection methods on chloride threshold value for the corrosion of steel reinforcement, Constr Build Mater., 23 (2009) 1902-1908.

[51] M. Moreno, W. Morris, M.G. Alvarez, G.S. Duffó, Corrosion of reinforcing steel in simulated concrete pore solutions: Effect of carbonation and chloride content, Corros. Sci., 46 (2004) 2681-2699.

[52] B. Kinsella, Y.J. Tan, S. Bailey, Electrochemical impedance spectroscopy and surface characterization techniques to study carbon dioxide corrosion product scales, Corrosion, 54 (1998) 835-842.

[53] C.-Q. Ye, R.-G. Hu, S.-G. Dong, X.-J. Zhang, R.-Q. Hou, R.-G. Du, C.-J. Lin, J.-S. Pan, EIS analysis on chloride-induced corrosion behavior of reinforcement steel in simulated carbonated concrete pore solutions, J. Electroanal. Chem., 688 (2013) 275-281.

[54] B.J. Usman, Z.M. Gasem, S.A. Umoren, M.M. Solomon, Eco-friendly 2-Thiobarbituric acid as a corrosion inhibitor for API 5L X60 steel in simulated sweet oilfield environment: Electrochemical and surface analysis studies, Sci. Rep., 9 (2019) 830.

[55] H. Herrera Hernández, F. González Díaz, G.D.J. Fajardo San Miguel, J.C. Velázquez Altamirano, C.O. González Morán, J. Morales Hernández, Electrochemical impedance spectroscopy as a practical tool for monitoring the carbonation process on reinforced concrete structures, Arabian Journal for Science and Engineering, 44 (2019) 10087-10103.

[56] R. Chen, J. Hu, Y. Ma, W. Guo, H. Huang, J. Wei, S. Yin, Q. Yu, Characterization of the passive film formed on the reinforcement surface in alkali activated fly ash: Surface analysis and electrochemical evaluation, Corros. Sci., 165 (2020) 108393.

[57] G. Brug, A. Van Den Eeden, M. Sluyters-Rehbach, J. Sluyters, The analysis of electrode impedances complicated by the presence of a constant phase element, J. Electroanal. Chem., 176 (1984) 275-295.

[58] L. Yohai, M.B. Valcarce, M. Vázquez, Testing phosphate ions as corrosion inhibitors for construction steel in mortars, Electrochimica Acta, 202 (2016) 316-324.

[59] H. Verbruggen, H. Terryn, I. De Graeve, Inhibitor evaluation in different simulated concrete pore solution for the protection of steel rebars, Constr Build Mater., 124 (2016) 887-896.

[60] I. Sekine, A. Masuko, K. Senoo, Corrosion behavior of AISI 316 stainless steel in formic and acetic acid solutions, Corrosion, 43 (1987) 553-560.

[61] B. Wang, L. Xu, J. Zhu, H. Xiao, M. Lu, Observation and analysis of pseudopassive film on 6.5%Cr steel in CO_2 corrosion environment, Corros. Sci., 111 (2016) 711-719.

[62] X. Li, S. Deng, H. Fu, Sodium molybdate as a corrosion inhibitor for aluminium in H_3PO_4 solution, Corros. Sci., 53 (2011) 2748-2753.

[63] M.A. Quraishi, S.K. Shukla, Poly(aniline-formaldehyde): A new and effective corrosion inhibitor for mild steel in hydrochloric acid, Materials Chemistry and Physics, 113 (2009) 685-689.

[64] Y. Wang, G. Cheng, W. Wu, Q. Qiao, Y. Li, X. Li, Effect of pH and chloride on the micro-mechanism of pitting corrosion for high strength pipeline steel in aerated NaCl solutions, Applied Surface Science, 349 (2015) 746-756.

[65] B. Huet, V. L'hostis, G. Santarini, D. Feron, H. Idrissi, Steel corrosion in concrete: Determinist modeling of cathodic reaction as a function of water saturation degree, Corros. Sci., 49 (2007) 1918-1932.

[66] M. Trueba, S.P. Trasatti, Study of Al alloy corrosion in neutral NaCl by the pitting scan technique, Materials Chemistry and Physics, 121 (2010) 523-533.

[67] B.E. Wilde, E. Williams, The use of current/voltage curves for the study of localized corrosion and passivity breakdown on stainless steels in chloride media, Electrochimica Acta, 16 (1971) 1971-1985.

[68] X. Feng, Y. Tang, Y. Zuo, Influence of stress on passive behaviour of steel bars in concrete pore solution, Corros. Sci., 53 (2011) 1304-1311.

[69] X. Feng, Y. Zuo, Y. Tang, X. Zhao, J. Zhao, The influence of strain on the passive behavior of carbon steel in cement extract, Corros. Sci., 65 (2012) 542-548.

[70] H. Luo, C.F. Dong, X.G. Li, K. Xiao, The electrochemical behaviour of 2205 duplex stainless steel in alkaline solutions with different pH in the presence of chloride, Electrochimica Acta, 64 (2012) 211-220.

[71] A. Grosvenor, B. Kobe, M. Biesinger, N. McIntyre, Investigation of multiplet splitting of Fe 2p XPS spectra and bonding in iron compounds, Surface and Interface Analysis, 36 (2004) 1564-1574.

[72] H. Dai, W. Xu, Y. Chen, M. Li, Z. Chen, B. Yang, S. Mei, W. Zhang, F. Xie, W. Wei, R. Guo, G. Zhang, Narrow band-gap cathode $Fe_3(PO_4)_2$ for sodium-ion battery with enhanced sodium storage, Colloids Surf. Physicochem. Eng. Aspects, 591 (2020) 124561.

[73] J.A. Dean, Lange's handbook of chemistry, New york; London: McGraw-Hill, Inc.1999.

[74] A.L. Iglesia, Estimating the thermodynamic properties of phosphate minerals at high and low temperature from the sum of constituent units, Consejo Superior de Investigaciones Científicas, 65 (2009) 109-119.

[75] T. Kodama, Formation of iron orthophosphate colloids and anodic films on iron in phosphate solutions, Corrosion Engineering, 23 (1974) 545-551.

[76] P. Vieillard, Y. Tardy, Thermochemical properties of phosphates, Phosphate minerals, Springer1984, pp. 171-198.

[77] K.B. Ayala-Luis, C.B. Koch, H.C.B. Hansen, The standard Gibbs energy of formation of Fe(II)Fe(III) hydroxide sulfate green rust, Clays Clay Miner., 56 (2008) 633-644.

[78] L. Bertolini, B. Elsener, P. Pedeferri, E. Redaelli, R.B. Polder, Corrosion of steel in concrete: prevention, diagnosis, repair, John Wiley & Sons2013.

[79] T.E. Pou, Passive films on iron: The mechanism of breakdown in chloride containing solutions, Journal of the Electrochemical Society, 131 (1984) 1243.

[80] J. Shi, J. Ming, W. Sun, Electrochemical performance of reinforcing steel in alkali-activated slag extract in the presence of chlorides, Corros. Sci., (2018).

[81] P. Refait, S.H. Drissi, J. Pytkiewicz, J.M.R. Génin, The anionic species competition in iron aqueous corrosion: Role of various green rust compounds, Corros. Sci., 39 (1997) 1699-1710.

[82] S. Das, M.J. Hendry, Application of Raman spectroscopy to identify iron minerals commonly found in mine wastes, Chemical Geology, 290 (2011) 101-108.

[83] M. Morcillo, B. Chico, J. Alcántara, I. Díaz, R. Wolthuis, D. de la Fuente, SEM/Micro-Raman characterization of the morphologies of marine atmospheric corrosion products formed on mild steel, Journal of The Electrochemical Society, 163 (2016) C426-C439.

[84] C. Rémazeilles, P. Refait, On the formation of β-FeOOH (akaganéite) in chloride-containing environments, Corros. Sci., 49 (2007) 844-857.

[85] M. Bouchard, D.C. Smith, Catalogue of 45 reference Raman spectra of minerals concerning research in art history or archaeology, especially on corroded metals and coloured glass, Spectrochimica Acta Part A: Molecular and Biomolecular Spectroscopy, 59 (2003) 2247-2266.

[86] O.N. Shebanova, P. Lazor, Raman spectroscopic study of magnetite ($FeFe_2O_4$): a new assignment for the vibrational spectrum, J. Solid State Chem., 174 (2003) 424-430.

[87] M.A. Legodi, D. de Waal, The preparation of magnetite, goethite, hematite and maghemite of pigment quality from mill scale iron waste, Dyes and Pigments, 74 (2007) 161-168.

[88] M. Criado, S. Martínez-Ramirez, J.M. Bastidas, A Raman spectroscopy study of steel corrosion products in activated fly ash mortar containing chlorides, Constr Build Mater., 96 (2015) 383-390.

[89] R.L. Frost, M.L. Weier, K.L. Erickson, O. Carmody, S.J. Mills, Raman spectroscopy of phosphates of the variscite mineral group, Journal of Raman Spectroscopy, 35 (2004) 1047-1055.

[90] N. Boucherit, A.H.-L. Goff, Localized corrosion processes in iron and steels studied by in situ Raman spectroscopy, Faraday Discuss., 94 (1992) 137-147.

[91] P.K. Katiyar, P.K. Behera, S. Misra, K. Mondal, Comparative corrosion behavior of five different microstructures of rebar steels in simulated concrete pore solution with and without chloride addition, J. Mater. Eng. Perform., 28 (2019) 6275-6286.

[92] J. Shi, J. Ming, Y. Zhang, J. Jiang, Corrosion products and corrosion-induced cracks of low-alloy steel and low-carbon steel in concrete, Cem. Concr. Compos., 88 (2018) 121-129.

[93] M. Liu, X. Cheng, X. Li, T.J. Lu, Corrosion behavior of low-Cr steel rebars in alkaline solutions with different pH in the presence of chlorides, J. Electroanal. Chem., 803 (2017) 40-50.

[94] Z. Ai, J. Jiang, W. Sun, D. Song, H. Ma, J. Zhang, D. Wang, Passive behaviour of alloy corrosion-resistant steel Cr10Mo1 in simulating concrete pore solutions with different pH, Applied Surface Science, 389 (2016) 1126-1136.

[95] K.S. Rajagopalan, K. Venu, K. Balakrishnan, Anodic polarization studies in neutral and alkaline solutions containing corrosion inhibitors, Journal of the Electrochemical Society, 109 (1962) 81.

[96] T. Yonezawa, V. Ashworth, R.P.M. Procter, Pore solution composition and chloride effects on the corrosion of steel in concrete, Corrosion, 44 (1988) 489-499.

[97] C. Giacomelli, F. Giacomelli, R. Bortolluzzi, A. Spinelli, Properties of potentiostatic passive films grown on iron electrodes immersed in weak - alkaline phosphate solutions, Anti-corros. method m., (2006).

[98] J. Antelo, M. Avena, S. Fiol, R. López, F. Arce, Effects of pH and ionic strength on the adsorption of phosphate and arsenate at the goethite–water interface, Journal of Colloid and Interface Science, 285 (2005) 476-486.

[99] S.M. Tawfik, N.A. Negm, Synthesis, characterization and evaluation of some anionic surfactants with phosphate group as a biodegradable corrosion inhibitor for carbon steel in acidic solution, J. Mol. Liq., 215 (2016) 185-196.

[100] R. Chitrakar, S. Tezuka, A. Sonoda, K. Sakane, K. Ooi, T. Hirotsu, Phosphate adsorption on synthetic goethite and akaganeite, Journal of Colloid and Interface Science, 298 (2006) 602-608.

[101] U.R. Evans, CXL.—The passivity of metals. Part I. The isolation of the protective film, Journal of the Chemical Society (Resumed), (1927) 1020-1040.

[102] H.M. Azam, K.T. Finneran, Fe(III) reduction-mediated phosphate removal as vivianite ($Fe_3(PO_4)_2 \cdot 8H_2O$) in septic system wastewater, Chemosphere, 97 (2014) 1-9.

[103] W. Khalil, S. Haupt, H.-H. Strehblow, The thinning of the passive layer of iron by halides, Mater. Corros., 36 (1985) 16-21.

[104] J. Shi, J. Ming, M. Wu, Electrochemical behavior and corrosion products of Cr-modified reinforcing steels in saturated $Ca(OH)_2$ solution with chlorides, Cem. Concr. Compos., 110 (2020) 103587.